WJSA-92-01
DOE/ER/54100-1

OSIRIS and SOMBRERO
Inertial Fusion Power Plant Designs

Volume 1
Executive Summary and Overview

Final Report
March 1992

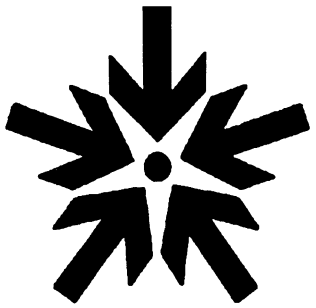

WJSA-92-01
DOE/ER/54100-1

OSIRIS and SOMBRERO
Inertial Confinement Fusion Power Plant Designs

Volume 1
Executive Summary and Overview

W. J. Schafer Associates
Wayne R. Meier, Robert L. Bieri, Michael J. Monsler,
Charles D. Hendricks, Paul Laybourne, Keith R. Shillito

Bechtel
Sunil K. Ghose, Lenard M. Goldman, Kim D. Auclair, Chan Y. Pang

General Atomics
Robert F. Bourque, Larry D. Stewart, Edward E. Bowles, Edward L. Hubbard

Textron Defense Systems
Chas. W. von Rosenberg, Jr., Malcolm W. McGeoch

University of Wisconsin
Igor N. Sviatoslavsky, Robert R. Peterson, Mohamed E. Sawan, Hesham Y. Khater,
Layton J. Wittenberg, Gerry L. Kulcinski, Gregory A. Moses, ElSayed A. Mogahed,
Joseph J. MacFarlane, Sean Rutledge

Accelerator Consultants
Stanley Humphries, Jr.

TSI Research
Edward T. Cheng

March 1992

Disclaimer

Acknowledgments

The authors would like to acknowledge the help in the form of briefings and discussions with individuals in the Inertial Confinement Fusion Programs at the Laboratory for Laser Energetics, Lawrence Livermore National Laboratory, Los Alamos National Laboratory, and the Navy Research Laboratory, and individuals in the Heavy Ion Fusion Program at Lawrence Berkeley Laboratory. We also thank the members of the Oversight Committee for assembling the Study Guidelines and for providing feedback at our progress review meetings. We thank the secretaries at our institutions for their assistance in preparing this report with special thanks to Barbara Lane at W.J. Schafer Associates for editing the final report. Finally, we thank the Department of Energy, Office of Fusion Energy for supporting this study under contract No. DE-AC02-90ER54100.

CONTENTS

VOLUME 1 – EXECUTIVE SUMMARY AND OVERVIEW

VOLUME 2 – DESIGNS, ASSESSMENTS, AND COMPARISONS

Executive Summary

EXECUTIVE SUMMARY

INTRODUCTION

Conceptual designs and assessments have been completed for two inertial fusion energy (IFE) electric power plants. The detailed designs and results of the assessment studies are presented in this report. Osiris is a heavy-ion-beam (HIB) driven power plant, and SOMBRERO is a Krypton-Fluoride (KrF) laser-driven power plant. Both plants are sized for a net electric power of 1000 MWe. Key design features and operating parameters are given in Table I.

OSIRIS POWER PLANT

Osiris Chamber Design

- The Osiris chamber features a flexible, porous carbon fabric first wall and blanket that contains the molten salt, Flibe, which serves as the tritium breeding material and primary coolant. The first wall radius at the nearest point to the target is 3.5 m.

- A thin layer of Flibe coats the first wall to protect it from x-ray and debris damage.

- A spray of Flibe at the cold-leg temperature (500°C) is injected at the bottom of the chamber to condense the Flibe that is vaporized with each pulse.

HIB Driver Design

- The HIB driver uses linear induction accelerator technology. Twelve beams of 3.8 GeV Xe^{+1} ions deliver a total of 5 MJ to an indirect drive target at a pulse repetition rate of 4.6 Hz.

- The driver is designed to carry the maximum transportable current at every point along the accelerator in order to minimize cost.

- The driver efficiency is 28%, and the power consumption is 82 MWe.

- The design is conservative in that it does not use beam combination, beam separation, or recirculation.

- High performance Nb_3Sn superconductors in the quadrupole focusing magnets improve performance and reduce cost.

Osiris Balance of Plant

- The reactor building is quite compact and features a movable shielding wall for access to the maintenance building.

- The power conversion system uses a double reheat rankine power cycle with a gross electric conversion efficiency of 45%. After accounting for driver and auxiliary power consumption, the net efficiency of the power plant is 40%.

SOMBRERO POWER PLANT

SOMBRERO Chamber Design

- SOMBRERO features a carbon/carbon first wall and blanket structure with a granular Li_2O breeding blanket. The Li_2O granules flow through the blanket region of the chamber and serve as the primary coolant.

- The first wall is protected from x-ray and debris damage by xenon gas at 0.5 torr.

- Low pressure He is used to remove tritium from the breeding blanket and also to transport the Li_2O granules to and from the intermediate heat exchangers.

KrF Laser Design

- The KrF laser uses e-beam pumped amplifiers and angular multiplexing for pulse compression. Sixty beams deliver a total of 3.4 MJ to a direct drive target at 6.7 Hz.

- The non-intercepting e-beam cathode technology promises long-life operation and improves the system efficiency.

- The laser design achieves an overall system efficiency of 7.5% and has a total power consumption of 304 MWe.

Power Conversion and BOP

- SOMBRERO requires a large (110 m diameter) reactor building to accommodate the final focusing optics for the laser. The entire building is a vacuum structure filled with 0.5 torr of xenon used for first wall protection.

- The sensitive dielectric optics are protected from neutron damage by the use of grazing incidence metal mirrors (GIMMs). While the lifetime of the dielectric optics is very uncertain, present assumptions indicate that they could last for the life of the power plant. The life of the GIMMs depends on the degree to which radiation damage can be annealed by heating.

- SOMBRERO uses the same intermediate coolant loop and steam power cycle as Osiris. The gross efficiency is 47% and includes a credit for using waste heat from the laser in the feedwater heaters. After accounting for laser and auxiliary power consumption, the net plant efficiency is 35%.

TARGET SYSTEMS

Target Production Facility

- The target production facility design uses controlled microencapsulation for shell production, cryogenic injection fill for fuel loading, and a combination of cold-gas jets and pulsed laser heating to establish a uniform fuel layer.

- The design is 100% redundant to improve reliability and minimize the need to store extra targets and the associated tritium inventory.

- The DT-fill and layering techniques minimize production time and thus minimize tritium inventory.

- The total estimated tritium inventory of the target factory is only 300 g.

Target Injection, Tracking, and Beam Pointing

- A gas gun injector accelerates targets at 130 g's over a distance of 9 m to a final velocity of 150 m/s.

- A laser Doppler interferometer and laser diode tracking stations measure the target trajectory and provide pointing information to the drivers.

- Active beam pointing is proposed for both the HIB and KrF-laser drivers.

ENVIRONMENTAL AND SAFETY ASPECTS

- Only low activation materials are used in the first walls, blankets, breeding materials, and chamber structures of both the Osiris and SOMBRERO designs.

- Both power plants achieve a Level of Safety Assurance of 1.

- Structures and shielding for both designs qualify for Class A shallow land burial. Osiris breeding material qualifies for Class A while SOMBRERO breeding material qualifies for Class C shallow land burial.

- Nuclear grade construction is not needed for either design.

MAINTAINABILITY

- The first wall and blanket structure for Osiris are removed as a single unit by first draining the blanket of Flibe and then lifting the internal components out the vacuum vessel with an overhead crane.

- The SOMBRERO chamber is constructed of 12 first-wall / blanket units. To replace a segment, it is lowered to a transport carriage and moved to the maintenance building.

TECHNOLOGY DEVELOPMENT NEEDS

- To realize the attractive features of these designs, technology development is needed in several areas.

- Driver technology should be given the highest priority in both cases. Beam delivery systems (heavy-ion-beam transport and final optics for lasers) are important research areas.

- Economical automated target production techniques are required for both designs.

- For Osiris, technology development and experiments are needed to prove the feasibility of the operation of the first wall protection scheme and chamber operation in a rep-rated mode.

- For SOMBRERO, the development of large-structures made of low activation material is needed.

ECONOMICS

- The estimated constant dollar cost of electricity (COE) for Osiris is 5.6 ¢/kWh, while the COE for SOMBRERO is 6.7 ¢/kWh. Both COEs compare favorably with reported COEs for magnetic fusion energy reactors.

CONCLUSIONS

- The conceptual designs developed in this study show the potential promise of IFE for electric power production. We have developed technically credibly concepts with environmental, safety, and economic characteristics that are every bit as attractive as magnetic fusion energy reactors designs. Realizing IFE potential will require continued research and development in the areas of target physics, driver technologies, heavy ion beam transport, laser optics, chamber phenomenology, low activation materials, and automated target production.

Table I. Key Design Features for Osiris and SOMBRERO

	Osiris	SOMBRERO
Driver		
Driver Energy (MJ)	5.0	3.4
Rep-Rate (Hz)	4.6	6.7
Driver Efficiency (%)	28.2	7.5
Target		
Type	Indirect Drive	Direct Drive
Target Gain	86.5	118
Yield (MJ)	432	400
Chamber Design		
First Wall Material	Woven Graphite Fabric	4-D C/C Composite
X-ray and Debris Protection	Liquid Flibe	3.25 torr-m of Xe
First Wall Radius, m	3.5	6.5
Estimated First Wall Life (fpy)	1.8	5
Breeding Material	Molten Flibe	Li_2O Granules
Tritium Breeding Ratio	1.24	1.25
Power Conversion System		
Primary Coolant	Flibe	He w/ Li_2O granules
Intermediate Coolant	Lead	Lead
Secondary Coolant	Water / Steam	Water / Steam
Power Conversion Eff. (%)	45	47
Power Balance		
Fusion Power (MW)	1987	2677
Total Thermal Power (MWt)	2504	2891
Gross Electric Power (MWe)	1127	1359
Driver Power (MWe)	82	304
Auxiliary Power (MWe)	45	55
Net Electric Power (MWe)	1000	1000
Net Plant Efficiency (%)	40	35
Environmental & Safety		
Waste Disposal Ratings	A	A & C
Level of Safety Assurance	1	1
Economics		
Cost of Electricity (¢/kWh)	5.6	6.7

Overview

CONTENTS

OVERVIEW

1.0 INTRODUCTION

1.1 BACKGROUND

The Inertial Fusion Energy (IFE) Reactor Design Studies were sponsored by the Department of Energy's Office of Fusion Energy. The results of the study conducted by the W. J. Schafer Associates (WJSA) team, which consisted of Bechtel, General Atomics (GA), Textron Defense Systems, and the University of Wisconsin, are reported here.

The primary objective of the IFE Reactor Design Studies was to provide the Department of Energy with an evaluation of the potential of inertial fusion for electric power production.[1] Conceptual designs were completed for two IFE electric power plants, one using an induction linac heavy ion beam (HIB) driver and the other using a Krypton Fluoride (KrF) laser driver. The two designs are the HIB-driven Osiris reactor and the KrF laser-driven SOMBRERO reactor. (SOMBRERO is an acronym for **SO**lid **M**oving **BRE**eder **R**eactor.)

These studies included the conceptual design and analysis of all aspects of the IFE power plants: the chambers, heat transport and power conversion systems, other balance of plant facilities, target systems (including the target production, injection, and tracking systems), and the two drivers. After the two point designs were developed, they were assessed in terms of their 1) environmental and safety aspects; 2) reliability, availability, and maintainability; 3) technical issues and technology development requirements; and 4) economics. Finally, we compared the design features and the results of the assessments for the two designs.

1.2 ORGANIZATION OF THE OVERVIEW

The main sections of the Overview correspond to the chapters of Volume 2 - Designs, Assessments, and Comparisons. Therefore, to get more detailed information on the topics described in the Overview, the reader is referred to the corresponding chapters in Volume 2.

Description of the Designs. Sections 2 to 4 contain brief descriptions of the designs. Section 2 is devoted to the Osiris HIB-driven power plant, Section 3 provides a description of the SOMBRERO laser-driven power plant, and Section 4 deals with the target systems for both plants.

Assessment of the Designs. Sections 5 to 8 are assessments of the designs. Section 5 covers the environmental and safety assessments for SOMBRERO and Osiris, Section 6 contains the reliability, availability, and maintainability (RAM) assessments, Section 7 summarizes the

technology development needs and priorities, and Section 8 summarizes the results of our economic assessment of the two designs.

Comparison of the Designs. Section 9 gives some of the key comparisons between the two designs.

Conclusions and Recommendations. Section 10 reproduces Chapter 10 from Volume 2 in its entirety.

2.0 OSIRIS HIB-DRIVEN POWER PLANT

2.1 SUMMARY OF OSIRIS PLANT PARAMETERS

Osiris is a 1000 MWe, HIB-driven power plant design. The Osiris Chamber is of the thick liquid-wall family, a descendent of HYLIFE,[2] HIBALL,[3] Pulse*Star,[4] and HYLIFE-II.[5] The Osiris chamber design features a porous carbon fabric blanket that is filled with the molten salt Flibe ($2LiF\text{-}BeF_2$). A key feature of Osiris is the use of low activation ceramics in a configuration in which brittleness and leak-tightness are not issues. A thin layer of liquid Flibe coats the carbon fabric first wall to protect it from x-ray and debris damage. Part of this protective layer is vaporized with each pulse. The vaporized Flibe condenses in a spray at the bottom of the chamber. Flibe circulates through the blanket and serves as the primary coolant and tritium breeding material. The blanket support structures and vacuum vessel are made of low activation carbon/carbon composites. Liquid lead is used in the intermediate loop to transfer heat to a steam generator and a double reheat steam power cycle.

The heavy ion driver uses singly-charged xenon ions. The design approach is conservative in that it does not use beam combination, separation, or recirculation. The design maximizes component standardization. It uses a propagation mode in the accelerator with constant beam radius, high-performance Nb_3Sn quadrupoles with constant strength and length, and a single quadrupole array configuration. There are only two inductor cell designs, one each for low and high energy. Illumination of the target is double-sided with six beams from each side.

The key plant operating parameters are listed in Table 2.1.

2.2 OSIRIS CHAMBER DESIGN

The Osiris chamber is shown in Fig. 2.1, and the key chamber design parameters are given in Table 2.2. The first wall and blanket are made of a flexible, woven carbon fabric that is stitched together much like a tent. To minimize stress on the fabric from the hydrostatic and pressure head of the Flibe, the fabric blanket is constructed like an air mattress, as shown in Fig. 2.2. Flibe enters the top of the chamber at 500°C and flows down the 5-cm-thick flow channel behind the first wall at a maximum velocity of 5 m/s. A small fraction of the Flibe flows through the porous fabric first wall to provide a protective liquid layer. The fabric weave is adjusted to control the flow rate through the first wall. The high flow rate in the first wall channel limits the temperature rise of the Flibe near the first wall. Therefore, the Flibe that weeps though the fabric to coat the

Table 2.1. Osiris Power Plant Operating Parameters

Driver Energy (MJ)	5.0
Target Gain	86.5
Target Yield (MJ)	432
Rep rate (Hz)	4.6
Fusion Power (MW)	1987
Energy Multiplication	1.26
Total Thermal Power (MW)	2504
Power Conversion Efficiency (%)	45
Gross Electrical Power (MWe)	1127
Driver Efficiency (%)	28
Driver Power (MWe)	82
Auxiliary Power (MWe)	45
Net Electric Power (MWe)	1000
Tritium Breeding Ratio	1.24

first wall is always near the cold-leg temperature. This helps maintain the low pressure conditions needed for beam propagation.

After flowing down the backside of the first wall, the Flibe coolant turns and flows upward, absorbing the neutron heat. It exits the blanket at the top and cascades down the outside with considerable turbulence, releasing some of the bred tritium to the vacuum system.

The target yield per pulse is 432 MJ. About 30% of this energy is in x-rays and debris and results in the vaporization of ~4.2 kg of Flibe from the protective layer. The impulse due to the blowoff was calculated to be 90 Pa-s at R = 3.5 m. Because the Flibe and carbon have comparable impedances, the kinetic energy from this blowoff will be distributed throughout the blanket. The kinetic energy is a negligible 0.05 J/m^2. Volumetric heating from the neutrons near the first wall is 5 J/cm^3, giving a temperature rise per pulse of only one degree.

With the tent-like geometry of the chamber, the blowoff vapor is preferentially directed toward the spray and pool at the bottom of the chamber. The 46 m/s spray is supplied with Flibe at the cold-leg temperature of 500°C to enhance condensation. The vaporized Flibe is "cryopumped" by the Flibe spray and pool down to the required $5x10^{18}$ $atoms/m^3$ in less than 60 ms, well below the 220 ms interpulse time. Because the vapor is condensed in the spray and pool, there is very little heat transfer through the first wall. Flibe from the pool and the Flibe from the neutron blanket drain from the bottom of the chamber with an average outlet temperature of 650°C.

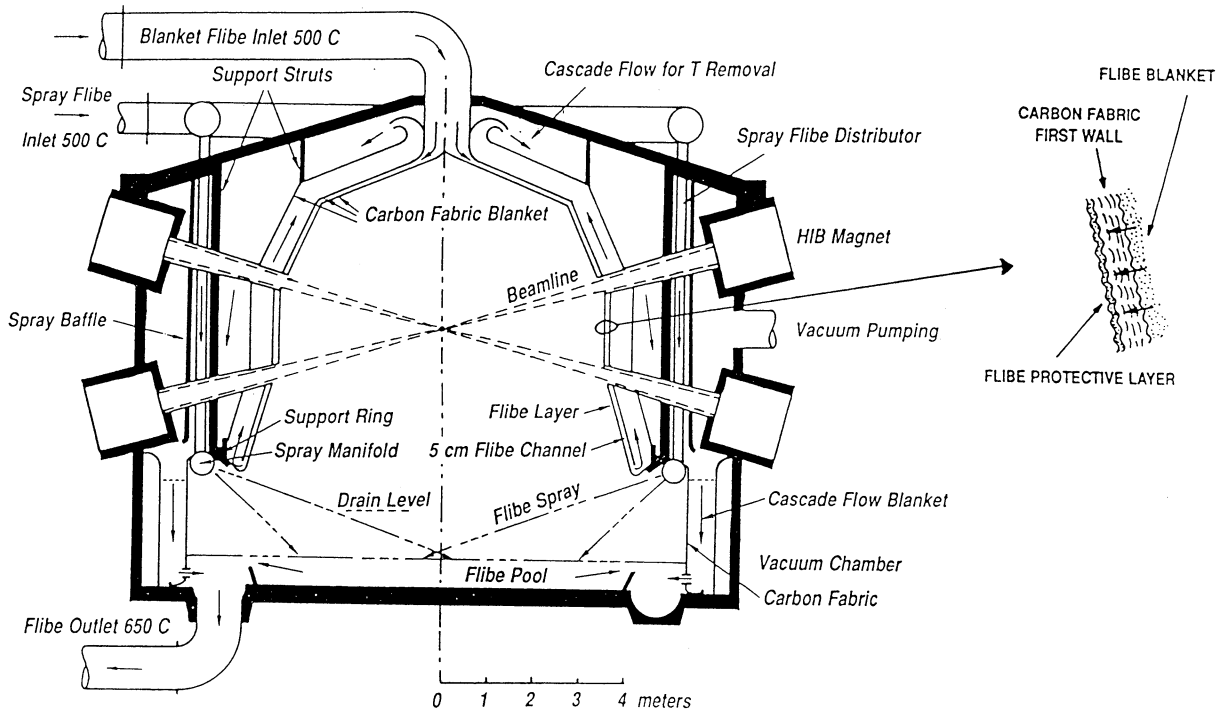

Fig. 2.1. Osiris chamber design.

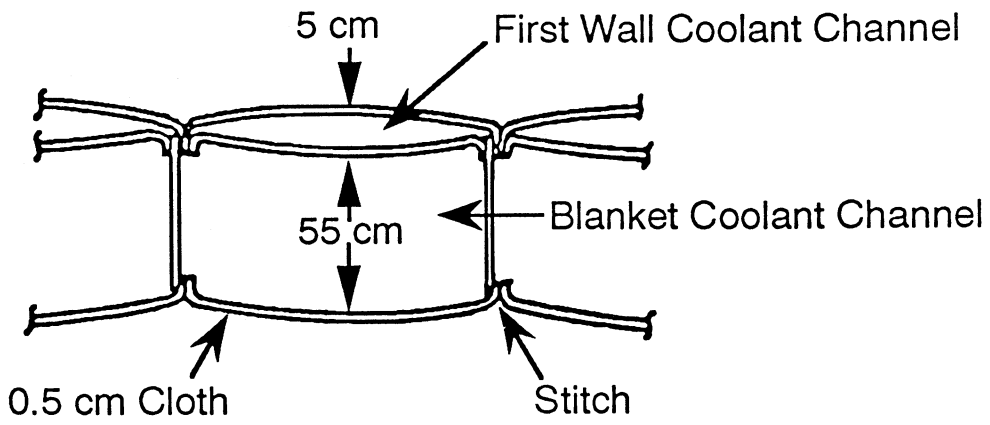

Fig. 2.2. Cross section of the carbon fabric blanket.

Table 2.2. Osiris Chamber Design Parameters

First Wall Radius at Midplane (m)	3.5
Flibe Vaporized per Shot (kg)	4.2
Peak Pressure on First Wall (GPa)	37
Impulse on First Wall (Pa-s)	90
Blanket Thickness (m)	0.7
Total Thermal Power (MW)	2504
Surface Power (MW)	596
Blanket Power (MW)	1908
Flibe Inlet Temperature (°C)	500
Flibe Outlet Temperature (°C)	650
Spray Flow Rate (kg/s)	2265
Blanket Flow Rate (kg/s)	4598
Max. First Wall Channel Velocity (m/s)	5
Flibe Upflow Average Velocity (m/s)	0.2
Spray Velocity (m/s)	46
Spray Manifold Pressure (MPa)	2.1
Spray Ideal Pumping Power (MW)	3
Total Flibe Mass in Chamber (kg)	456,000
Total Supported Mass (kg)	274,000
Main Support Hanger Diameter (m)	0.1
Number of Hangers	24
Hanger Tensile Stress (MPa)	14
Total Flibe Inventory (kg)	940,000

The Osiris blanket has excellent neutronic performance in terms of tritium breeding and energy multiplication. The reference design has a 60-cm-thick main blanket plus 10 cm cascade flow along the outside of the blanket. This gives a tritium breeding ratio of 1.24 with 1.10 coming from ^{6}Li. The energy multiplication factor is 1.26, which boosts the 1987 MW of fusion power to 2504 MW of total thermal power. The displacement damage rate in the carbon fabric first wall is about 42 dpa/full power year (fpy), and the helium production rate is about 1100 appm/fpy. While the damage limits for the carbon fabric are uncertain, we estimated a first wall life of 1.8 fpy. The maintenance scheme for the Osiris first wall, however, is very simple and should

not significantly increase the down-time of the power plant. The entire fabric assembly, drained of Flibe, is lifted out the top and replaced with a new assembly.

The vacuum vessel for Osiris is constructed of a low-activation carbon/carbon composite and is at a radius of ~6.5 m. The Flibe blanket effectively reduces the radiation damage and helium production rates to the composite vacuum vessel wall to 0.2 dpa/fpy and 10 appm/fpy, respectively. This component is, therefore, expected to last the full 30 year life of the plant.

2.3 OSIRIS POWER CONVERSION AND PLANT FACILITIES

2.3.1 Heat Transport System

The primary coolant for Osiris is liquid Flibe. Flibe enters the chamber at 500°C and exits at 650°C. The primary loop consists of two coolant circuits including one intermediate heat exchanger (IHX) in each circuit. Two circuits are used to keep the size of the IHXs from getting too large.

An intermediate coolant loop is used to isolate the primary coolant, which will contain radioactive elements, from the steam cycle. The intermediate loop consists of two circuits including one steam generator in each circuit. Liquid lead, operating between 400 and 600°C, is the intermediate coolant. It offers a safety advantage over sodium, which was considered as a possible alternative. While modest technology extrapolation is needed for the steam generators, their size appears to be reasonable.

To achieve a high efficiency power conversion, a high pressure/high temperature steam cycle is used. The steam pressure and temperature conditions chosen are consistent with the intermediate coolant temperature. These conditions also represent the state-of-the-art steam conditions used for fossil-fired steam power plants. A double-reheat steam cycle is used with the peak steam pressure and temperature of 24.2 MPa (3500 psig) and 538°C (1000°F), respectively. These conditions provide a power conversion efficiency of 45%.

There are two steam generators, and each is sized to handle half of the plant thermal output. Thus the thermal rating of each steam generator is 1250 MWt. To accommodate the double reheat feature of the power cycle, each steam generator is made up of three separate vessels: superheater, first reheater, and second reheater. These steam generator vessels are supplied with liquid lead from the IHXs.

The reactor plant is provided with a turbine-generator capable of generating 1127 MWe gross electrical power. The turbine-generator is a state-of-the-art design consisting of one high-pressure section, one intermediate-pressure section, and two low-pressure sections arranged in a cross-compound configuration.

2.3.2 Reactor Building

The reactor building provides housing for the reactor and shielding of the public from fusion neutrons. In addition, the building also accommodates remote maintenance of the reactor. The reactor building size is dictated by the maintenance handling requirements for the vacuum vessel cover and reactor internals. The conceptual arrangement of the building is shown in Figs. 2.3 and 2.4. The reactor is located at the center of the reactor hall. The IHXs are located in a separate hall so that the area can be accessed for limited periods during normal power operation; the reactor hall is provided with requisite shielding for this purpose. The nearest shielding wall is 10 m from the center of the chamber, and the shield thickness is 3.2 m.

Another feature of the reactor building is that there is no direct piping penetration between the reactor and IHX halls. The primary coolant piping is routed via an underground piping tunnel; there is no direct neutron path from the reactor hall to the IHX hall. The shield wall of the IHX hall is 1 m thick to allow unlimited access to the steam generator building.

2.4 HEAVY-ION DRIVER DESIGN

2.4.1 Summary of Results

The base 5-MJ heavy-ion induction driver design uses conservative design assumptions and has an efficiency of 28% and a direct cost of only $120/J. Combining the driver efficiency with an estimated target gain of 86.5 gives a recirculating power fraction for a 1000 MWe plant of only ~7%. We created a high-performance, low-cost design by

- using an original design for compact arrays of high-performance, Nb_3Sn quadrupoles that leads to small sizes and costs for the inductor cells as well as for the focusing arrays, and
- conducting a parametric search over a wide range of possible driver parameters to choose parameters that give an attractive design.

We use minimal extrapolation from existing accelerator technology and physics to create highly credible driver performance. We do not use any bends in the accelerator, beam combination, or beam separation. Although driver designs with bends, such as recirculating induction accelerators, offer the potential for cost savings by bending the beams in a circle and reducing the number of required driver elements, present performance uncertainties are large for high-current circular accelerators. Linear driver costs and projected target gains could be improved by combining beams early in the driver and separating them before final focusing; again we avoid performance uncertainties by not using beam combination or separation.

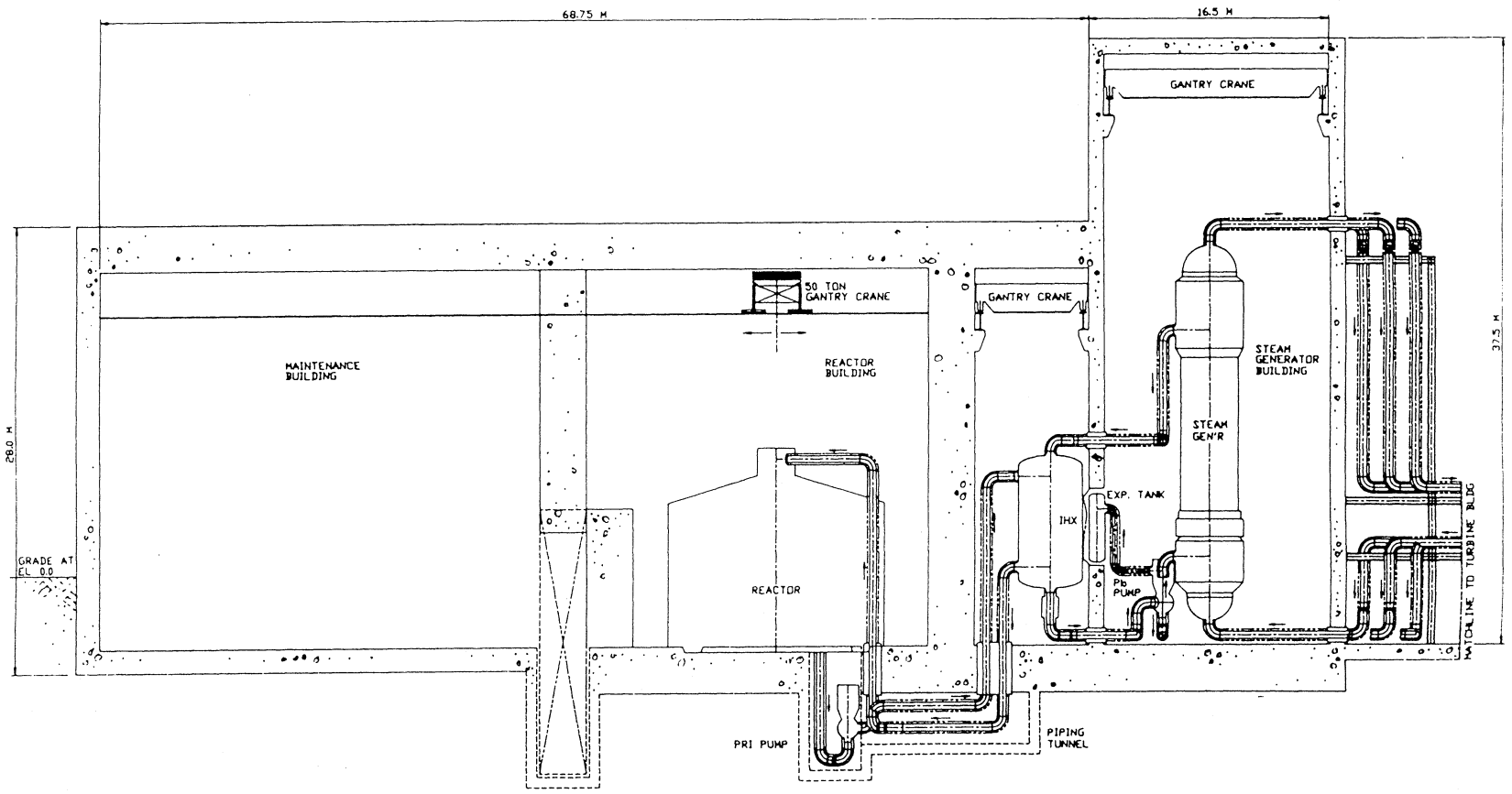

Fig. 2.3. Elevation view of Osiris reactor and steam generator buildings.

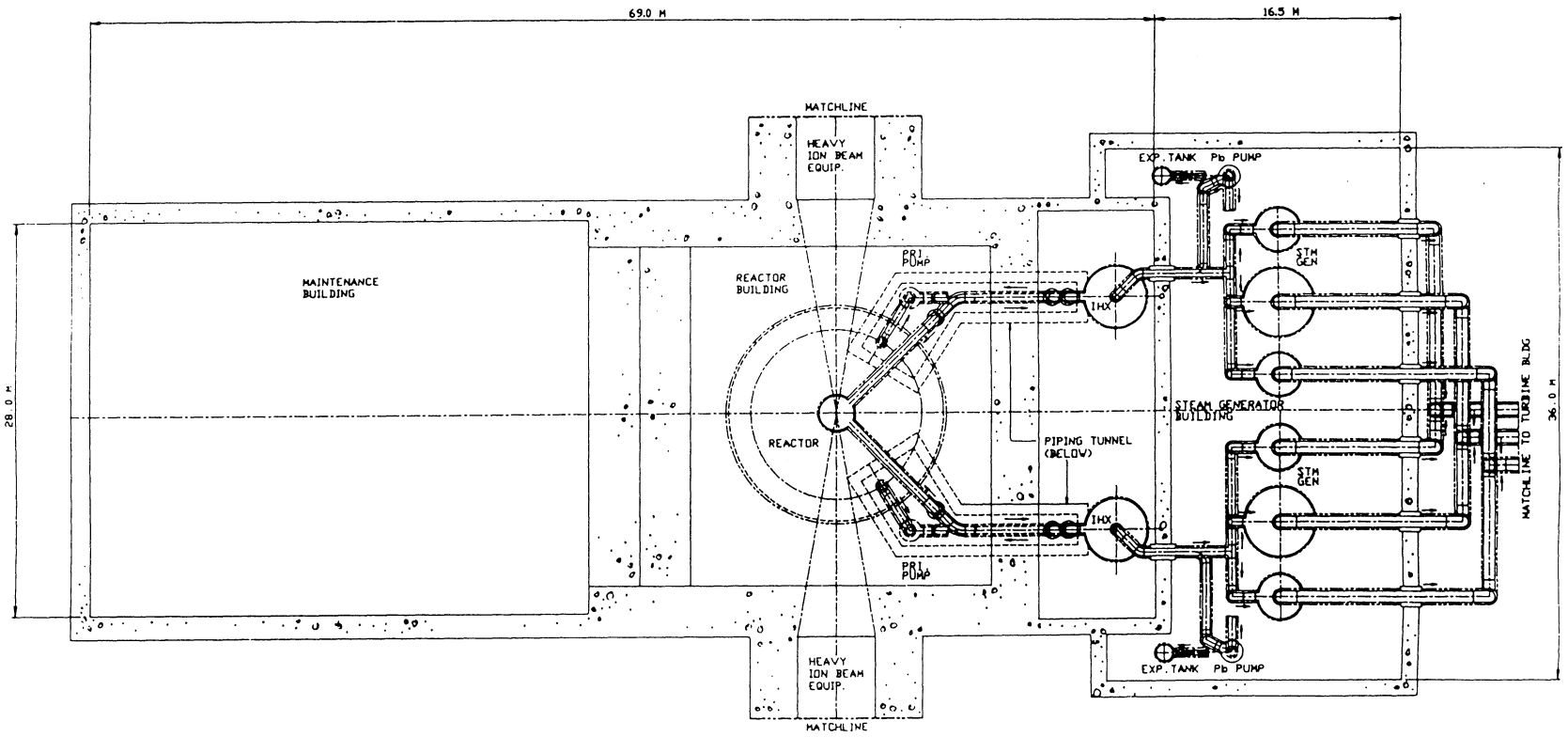

Fig. 2.4. Plan view of Osiris reactor and steam generator buildings.

We found significant cost savings by choosing our driver parameters after an extensive search of the allowed driver design parameters. Driver parameters varied in our design study were

- the number of beams in the driver,
- the ion mass,
- the ion charge state,
- the quadrupole focusing field strength,
- the quadrupole spacing, and
- the type of superconductor used in the quadrupole windings (Nb-Ti or Nb_3Sn).

We examined the effect of variations in each of these driver parameters on both the driver cost and projected target gain.

We have developed powerful tools for modeling a wide variety of drivers and identified several areas where these tools could be used to quantify the benefits resulting from possible design variations and more aggressive design options.

2.4.2 General Description of the Driver

The heavy-ion induction linac for use as a driver for the Osiris power plant consists of an ion injector, a multiple beam induction accelerator to produce high beam energies and currents, a drift compression region for shortening the ion bunch lengths, and a final focusing system for reducing the beam radii to the small spot size required for target ignition.

The injector consists of a source of charged ions and a voltage gradient to accelerate the ions. The injector is followed by an injection matching section where the ion beam parameters are adjusted to match those of the accelerator focusing lattice. There are several types of sources and injectors. A simple injector could consist of a plasma-discharge ion source followed by a voltage grid. In this design, ions would be created from a gas or vapor by a discharge voltage and then accelerated between electrical voltage grids. The shape of the grids (anodes and cathodes) is designed to produce a source of ions with minimal angular divergence. We have not created a detailed design of the injector, but we have used common limits to scale the achievable injection currents with ion mass, ion charge state, and acceleration gap voltage.

The accelerator consists of a lattice of quadrupole arrays with induction cells located between the arrays. The quadrupole arrays contain a superconducting quadrupole winding around each beam tube. The quadrupole fields of adjacent quadrupoles are offset by a 90° rotation to provide an alternating focusing lattice (which is described as a focusing-drift-defocusing-drift, or FODO, lattice). Each pair of quadrupoles in a repeating FODO lattice focuses the beam in two dimensions. Inductor cells are placed between quadrupoles as shown in Fig. 2.5. Each induction cell consists of a ferromagnetic core surrounding all of the beams as shown schematically in Fig. 2.6; the cores accelerate the beams through transformer action.

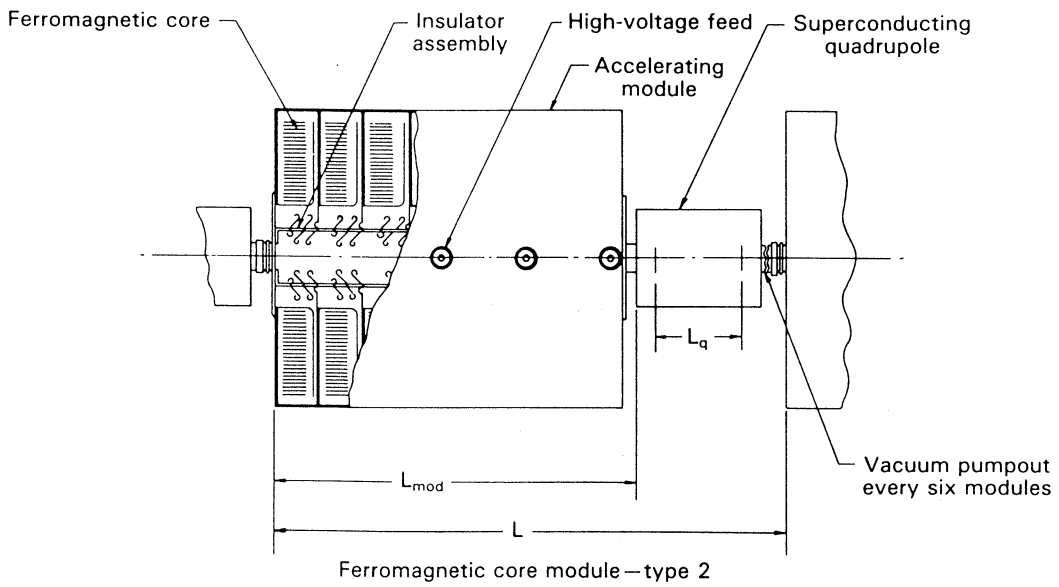

Fig. 2.5. Acceleration and focusing components in each half-lattice period.[6]

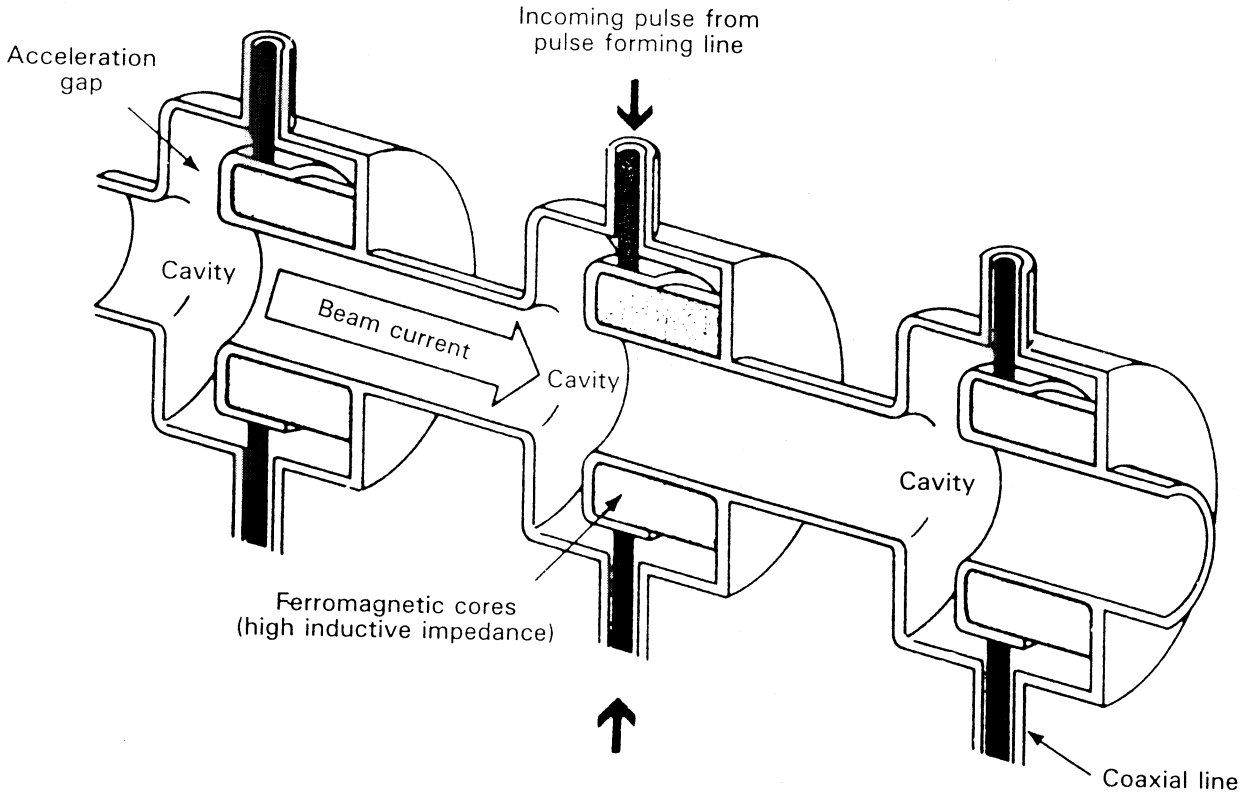

Fig. 2.6. Schematic cutaway of an induction linac.[7]

Because of the need for very short pulse durations at the target, the axial length of the pulse that comes out of the accelerator is shortened in a drift compression stage. The acceleration cells preceding the drift compression stage use shaped pulses to create a velocity tilt between the ions at the beginning and end of the pulse; this velocity tilt compresses the beam length until the velocity tilt is canceled by space-charge effects just before the beam reaches the target.

The final focusing system consists of quadrupole pairs or triplets which compress the beams to the final spot size. In order to attain the smallest possible spot sizes, the beams are spread and expanded before final focusing. The beams are also neutralized with co-injected electrons just after leaving the final focusing magnets in order to minimize space-charge effects during focusing.

Our design strategy builds upon one described by Monsler in 1987.[8] The chosen high-energy propagation mode uses a constant effective focusing length for each quadrupole and a constant beam radius. This allows for a single quadrupole array design to be used for the entire length of the driver. The spacing of the quadrupole arrays (the linear quad packing fraction) is varied so that the beam carries the maximum allowable current at every point in the driver.

Two types of inductor cells are used. A large radial build is used in the beginning of the driver where cores and quad arrays are packed closely together, and a smaller radial build is used in the high-energy section of the driver where there are greater separations between quad arrays. The use of inductors with a smaller radial build in the longest section of the driver lowers the total required volume of core material (Metglas).

The use of a single design for the quad arrays and only two designs for the inductors simplifies manufacturing requirements and allows for maximum economy of scale for producing driver components.

Our reference design is conservative in several respects. More aggressive driver designs use beam combination, beam separation, and/or recirculation to lower driver costs. All three modifications add performance uncertainties and design complexity, so we have chosen not to use these options in our base driver. We also chose a base design using singly charged, $q = 1$, ions. Higher charge states require more complicated sources and injectors, and highly charged ions may require better vacuums because of the increased potential for beam-gas charge exchange.

2.4.3 Accelerator Design

The base design for a 5 MJ accelerator was chosen after several parametric variation studies. The optimum value for each driver parameter depends on the chosen value of all the other variables, so an iterative approach was used to set the base parameters. The chosen driver parameters led to a 4.8 km long driver shown in Fig. 2.7. The driver parameters for this base design are shown Table 2.3.

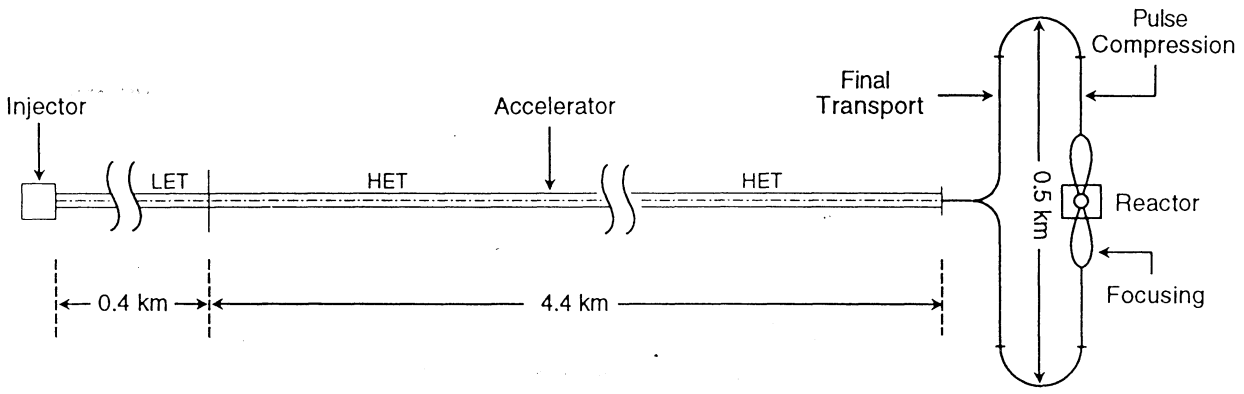

Fig. 2.7. Base heavy-ion driver schematic.

Table 2.3. Reference Parameters for HIB Driver Design

Energy (MJ)	5	Final Focus Half-angle (mrad)	33
Ion Mass (amu)	131	Spot Radius (mm)	2.3
Charge State	1	Ion Range (g/cm^2)	0.07
Superconductor	Nb_3Sn	Quads	
Number of Beams	12	Max. Axial Quad. Occupancy	0.8
B-max at S/C (T)	10	Number of Arrays	1978
Driver Efficiency (%)	28.2	Number of Quads	23,736
Beam Voltage		Effective Field Length (cm)	18.1
Initial (MV)	3	Quad Length (cm)	22.6
Final (GV)	3.83	Beam Radius (cm)	6.8
Current per Beam		Quad Bore (cm)	8.9
Initial (A)	3.5	LET Cores	
Final (kA)	1.09	Number	804
Pulse Length		Length (cm)	20
Initial (ms)	34	Radial Build (cm)	80
Final (ns)	100	HET Cores	
Accelerator Length		Number	6840
Low Energy (m)	359	Length (cm)	10
Pulse Matching (m)	33	Radial Build (cm)	40
High Energy (km)	4.4	Total Metglass (MT)	14.3
Total Length (km)	4.8		

2.4.4 Final Transport Design

The final compression and focus segment matches the 3.83 GeV Xe^{+1} linac output beam to the parameters specified at the target. Figure 2.8 shows the layout of the final compression and focus. There is a series of three functional sections: a transport section, a compression section, and a transverse focus section. The design illustrated in Fig. 2.8 allows the use of a conservative value (51.6 m) for the average bending radius. Also, the chosen layout eliminates the problem of dispersion in the bends due to the large coherent velocity tilt of the compression phase. Overall design parameters for final compression and focus are listed in Table 2.4. Each of the three functional sections of the final transport systems is described in the following paragraphs.

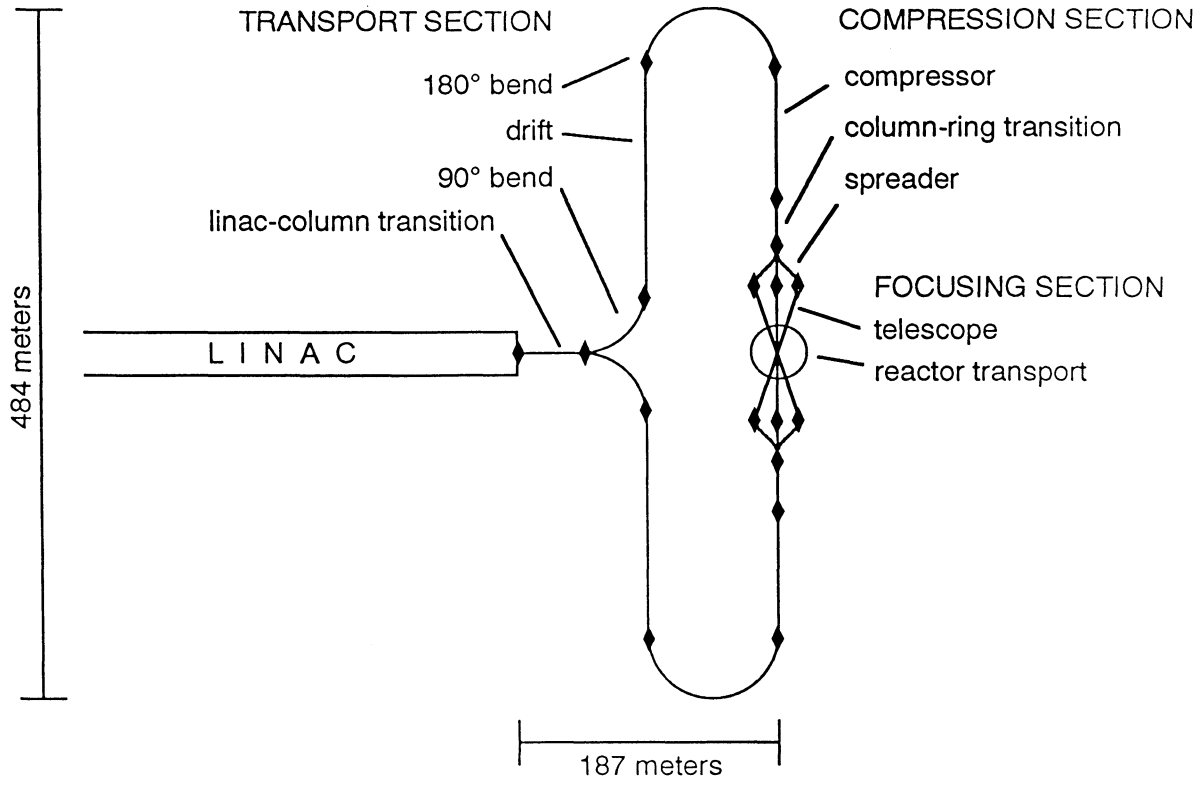

Fig. 2.8. Final compression and focus layout.

Table 2.4. Final Compression and Focus Design Parameters

Parameter	Value
Transport Length (m)	611
Linac-to-Target Distance (m)	187
Total Width ($\perp$ to linac) (m)	484
Number of Quadrupoles	984
Number of Dipoles	528

Transport Section. The transport section splits the 12-beam bundle from the linac into two 6-beam bundles, then transports each of the 6-beam bundles so that they are aimed at the target from a sufficient distance to accommodate compression and transverse focus. The transport section is composed of four elements: an initial transition element to transform the 12-beam bundle into two 6-beam columns, a 90 degree bend to direct the columns away from the linac axis, a straight section to carry the columns the required distance from the axis, and a 180 degree bend to direct the bundles back towards the target.

Compression Section. The compression section provides the specified 10 ns longitudinal focus in the middle of the final focusing quadrupole set. The compression section is comprised of three elements: the compressor element to provide the required velocity tilt, a transition element to transform the 6-beam column into a hexagonal ring, and a spreading element to provide sufficient clearance between the beams so that the final focusing quads of adjacent beams can be packaged.

Pulse shaping to provide a pre-pulse at the target would be done by tailoring the applied voltage gradient waveform in the compressor. This approach allows an arbitrary fraction of the pulse energy to be in the pre-pulse while preserving the equivalence of the individual beams.

Transverse Focus Section. The transverse focus section delivers the longitudinally-compressed beam to the target. It consists of two elements: a focusing telescope, which provides the required convergent angle to the beam bunches, and a reactor transport element, which provides the final beam steering and the auto-neutralizing electrons immediately before the beam bunches enter the reactor chamber. Some combination of shielding, baffles, and shutters at the reactor interface must be included to protect the final focusing components from target radiation, target debris, and hot molten Flibe.

3.0 SOMBRERO KRF-LASER DRIVEN POWER PLANT

3.1 SUMMARY OF SOMBRERO PLANT PARAMETERS

SOMBRERO is a 1000 MWe, KrF-laser driven power plant design. The SOMBRERO chamber is constructed of a low-activation carbon/carbon (C/C) composite. The first wall is protected with 0.5 torr of xenon buffer gas. Solid Li_2O particles flow by gravity through the blanket as the primary coolant and breeding material. This moving bed solid breeder blanket design has all the advantages of solid breeders but none of the disadvantages, such as the need for a high pressure gas coolant and a separate He gas loop for tritium extraction. Previous flowing solid breeder designs include a tokamak,[9] SOLASE,[10] and Cascade.[11] Helium is used to fluidize the particles for transport around the heat transfer loop. Liquid lead is used in the intermediate loop to transfer heat to a steam generator and a double reheat steam power cycle.

The KrF driver uses e-beam pumped amplifiers and angular multiplexing for pulse compression. The laser uses relatively small (~60 kJ) final amplifiers and a new plasma cathode technology for the e-beams in order to improve the laser system efficiency. Amplifiers are grouped in four-unit modules to minimize hardware requirements. Sixty beams are used to provide uniform target illumination. Grazing incidence metal mirrors are used as the final optical component to remove the dielectric focusing mirrors from the direct line of sight of high energy neutrons.

The key plant operating parameters are listed in Table 3.1.

3.2 SOMBRERO CHAMBER DESIGN

A cross section of the SOMBRERO chamber is shown in Fig. 3.1, and the key design parameters are given in Table 3.2 The chamber is assembled from 12 wedge-shaped, carbon/carbon composite modules that are totally independent of each other with separate Li_2O inlet and outlet tubes. The chamber has a cylindrical central section with conical ends, a radius of 6.5 m at the midplane, and an overall height of 18 m. Each module is subdivided both radially and circumferentially into coolant channels as shown in Fig. 3.2 The carbon structure fraction increases from 3% at the front to 50% at the rear of the blanket, thus providing an integral reflector which does not require separate cooling. The first wall (FW) thickness is 1.0 cm. The thickness of the coolant channel behind the FW varies from 7 cm at the midplane to 37 cm at the upper and lower extremities, making the flow area constant along the entire FW from top to bottom. This is done to ensure a constant velocity at the FW where a high heat transfer coefficient is needed.

Table 3.1. SOMBRERO Power Plant Operating Parameters

Driver Energy (MJ	3.4
Target Gain	118
Target Yield (MJ)	400
Rep Rate (Hz)	6.7
Fusion Power (MW)	2677
Energy Multiplication	1.08
Total Thermal Power (MW)	2891
Power Conversion Efficiency (%)	47
Gross Electrical Power (MWe)	1359
Driver Efficiency (%)	7.5
Driver Power (MWe)	304
Auxiliary Power (MWe)	55
Net Electric Power (MWe)	1000
Tritium Breeding Ratio	1.25

Table 3.2. SOMBRERO Chamber Design Parameters

First Wall Radius at Midplane (m)	6.5
Overall Internal Height (m)	18
First Wall Thickness (cm)	1.0
Maximum Stress in First Wall (MPa)	43
Blanket Thickness (m)	1.0
Total Thermal Power (MW)	2981
Surface Power (MW)	803
Blanket Power (MW)	2088
Li_2O Inlet Temperature (°C)	550
Li_2O Avg. Outlet Temperature (°C)	740
Li_2O Flow Rate (kg/s)	5590
Max Li_2O Velocity at FW (m/s)	1.15
Number of Blanket Modules	12
Structural Mass Per Module (Tonne)	37.8
Number of Beam Ports	60
Li_2O Mass in Chamber (kg)	670,000
Total Li_2O Inventory (kg)	2,000,000

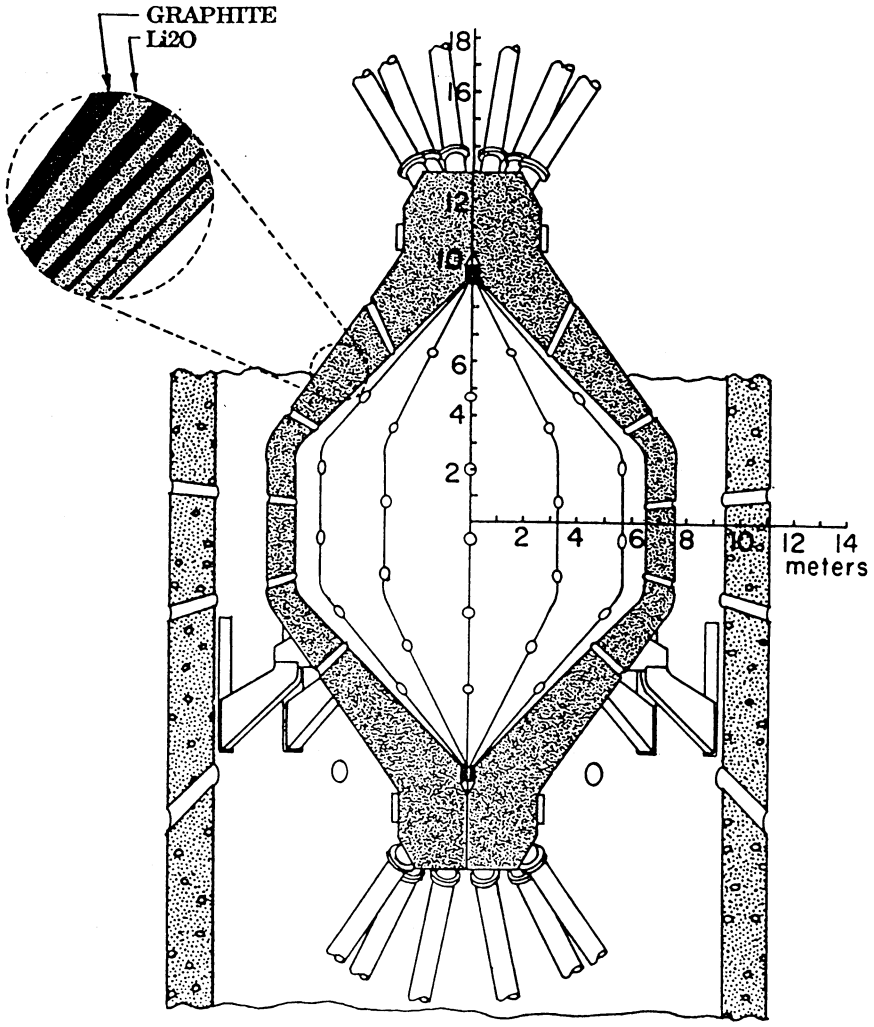

Fig. 3.1. Cross section of SOMBRERO Chamber.

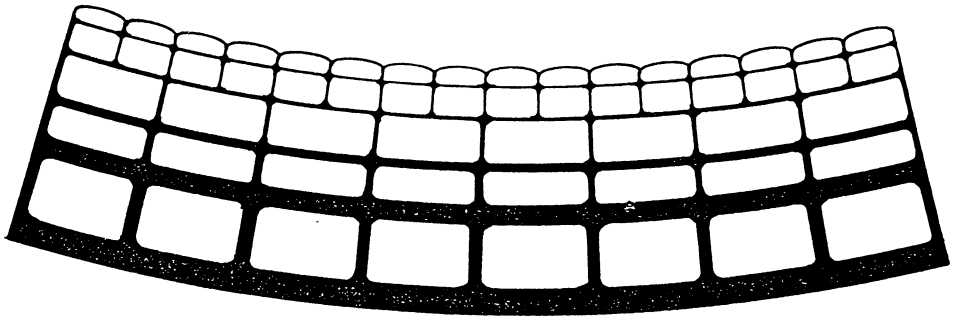

Fig. 3.2. Cross Section of SOMBRERO Blanket.

The Li_2O particles with a size range of 300-500 μm have a void fraction of 40% in the moving bed, and the grains are 90% of theoretical density. The Li_2O particles enter the top of the chamber from a manifold that doubles as a cyclone separator to remove the particles from the He gas that is used to transport Li_2O through the intermediate heat exchanger (IHX). After the particles enter the chamber, they flow under the force of gravity through the chamber and exit at the bottom. The Li_2O velocity at the FW is 1.15 m/s, and each succeeding radial zone has progressively lower velocities toward the rear of the blanket. Low pressure (0.2 MPa) He gas flows counter-current to the particles in the chamber coolant channels; this helps maintain a steady movement of the particles and prevents the formation of clustering or compaction. A thin coating of SiC on the inner surface of the coolant channels aids in sealing the C/C composite structure against He gas leakage into the chamber. The Li_2O inlet temperature to all the zones is 550°C, but the outlet temperature is 700°C for the FW coolant channel and 800°C for the rear zones. The total mass flow rate of 2×10^7 kg/hr has an equilibrated outlet temperature of 740°C. Flow in the different zones is controlled with baffles located at the bottom of the chamber to ensure that there will be no voids in the blanket. After going through the chamber, the particles are transported around the loop and through the IHX in a fluidized or entrained state by He gas.

The FW is protected from x-rays and ions by 0.5 torr of Xe gas. Since the beam ports are open to the reactor building, the whole building also has 0.5 torr of Xe gas. A certain amount of He leakage into the building can be tolerated without degrading the reactor performance. Innovative ideas for separating He from Xe, such as diffusion membranes, must be incorporated into the Xe recycling system.

SOMBRERO also has very good neutronic performance. The tritium breeding ratio is 1.25 with 0.91 coming from ^6Li. The energy multiplication factor is 1.08, which increases the 2677 MW of fusion power to 2891 MW of total thermal power. The peak displacement damage rate in the carbon first wall is about 15 dpa/fpy, and the helium production rate is about 3800 appm/fpy. The lifetime limit for radiation damage is uncertain. We assume that a materials program can develop a C/C composite with a damage limit of 75 dpa, which would give a first wall lifetime of ~ 5 fpy.

3.3 SOMBRERO POWER CONVERSION AND PLANT FACILITIES

3.3.1 Heat Transport System

The primary coolant for SOMBRERO is a flowing bed of Li_2O particles in He gas and operates between 550 and 740°C. The primary loop consists of four coolant circuits including one IHX in each circuit. The number of circuits is based on the size of the heat exchangers. A state-of-the-art heat exchanger design is assumed. An intermediate loop, with lead coolant operating

between 400 and 600°C, is used to isolate the SOMBRERO chamber from the high pressure steam loop. The coolant parameters are the same as in the case of Osiris.

3.3.2 Power Conversion

To achieve a high efficiency power conversion, a high pressure, high temperature steam cycle, similar to the Osiris plant, was adopted for the SOMBRERO plant. The steam conditions are the same as for the Osiris plant, with a peak pressure of 24.2 MPa and peak temperature of 538°C. As previously noted, these conditions provide a thermal conversion efficiency of 45%. However, in the case of SOMBRERO, 230 MWt of laser waste heat is used for feedwater heating, and this increases the cycle efficiency to 47%.

There are two steam generators, and each is sized for 50% of the thermal capacity (1490 MWt). The steam generator arrangement is similar to that of the Osiris plant. Each steam generator is made up of three separate vessels: superheater, first reheater, and second reheater.

The reactor plant is provided with a turbine-generator capable of generating 1360 MWe gross electrical power. Each turbine-generator is a state-of-the-art design consisting of a high-pressure section, an intermediate-pressure section, and two low-pressure sections arranged in a cross-compound configuration.

3.3.3 Reactor Building

A concept for the SOMBRERO reactor building has been developed. The building provides housing for the reactor, shielding of the public from fusion neutrons, and housing for the final optics. In addition, the building accommodates remote maintenance of the reactor. The concept for this building is shown in Figs. 3.3 and 3.4.

The size of the reactor building is dictated by the requirements for housing the final optics of the laser driver. It accommodates 60 beam lines that offer a near-uniform illumination. All the beam lines penetrate the reactor building through a beam handling area in the basement. The building vacuum boundary is located at the building floor where the beam lines penetrate the floor through windows.

The layout of the final optics is determined by the requirement for reasonable lifetimes of the final optics, which is highly uncertain since there are almost no data on radiation damage of either metal or dielectric optics in high neutron fluences. Grazing incidence metal mirrors (GIMM) made of aluminum are used to bend the beams slightly (84° angle of incidence) so that the dielectric focusing mirrors are out of the direct line of sight of fusion neutrons. The GIMMs are located 30 m from the center of the chamber, and the dielectric focusing mirrors are 50 m from the center of the chamber. Neutron dumps are located behind the GIMMs to further reduce the neutron flux experienced by the dielectric optics, which are expected to survive for the life of the plant without

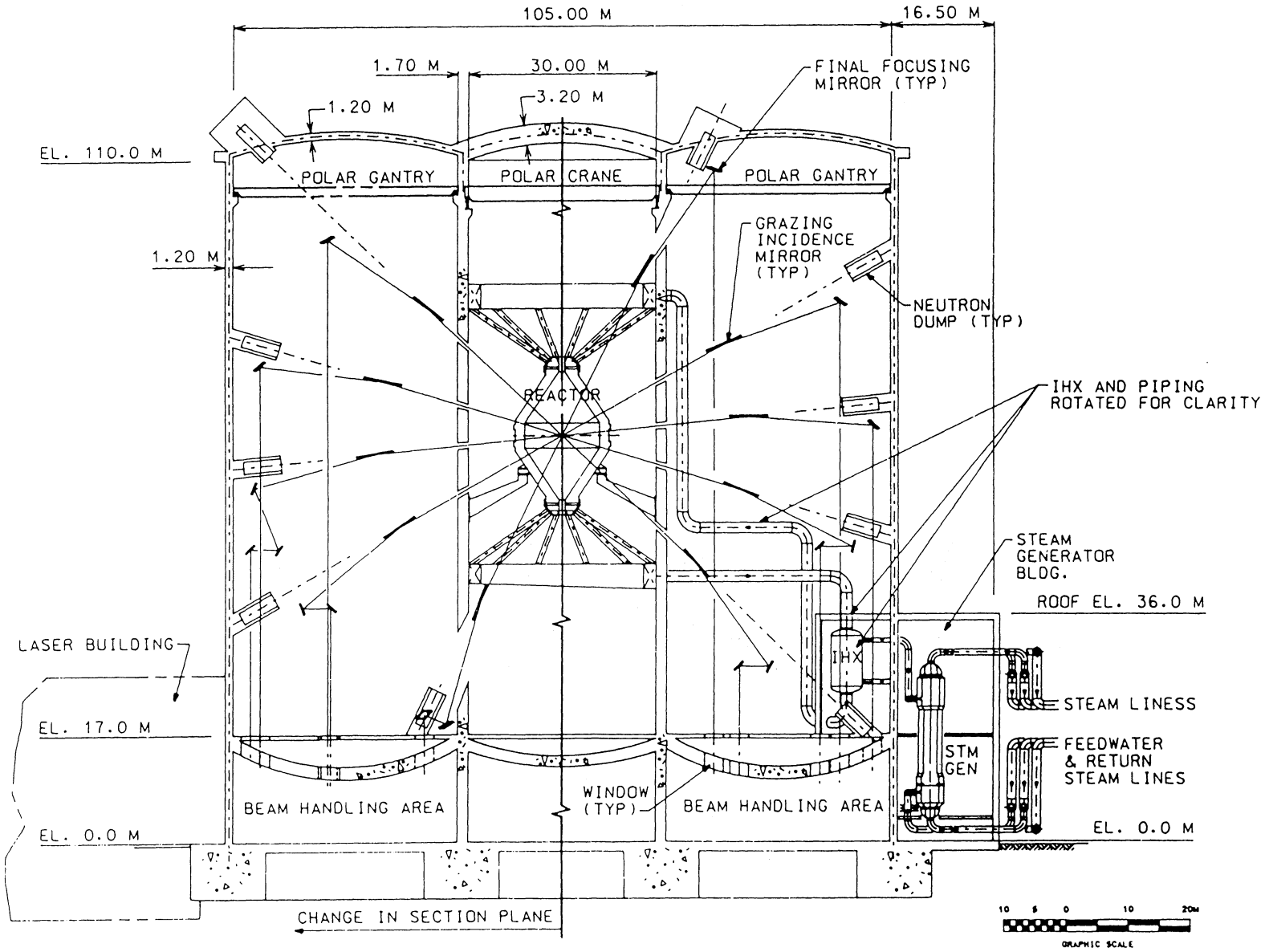

Fig. 3.3. Elevation view of the SOMBRERO reactor and steam generator buildings.

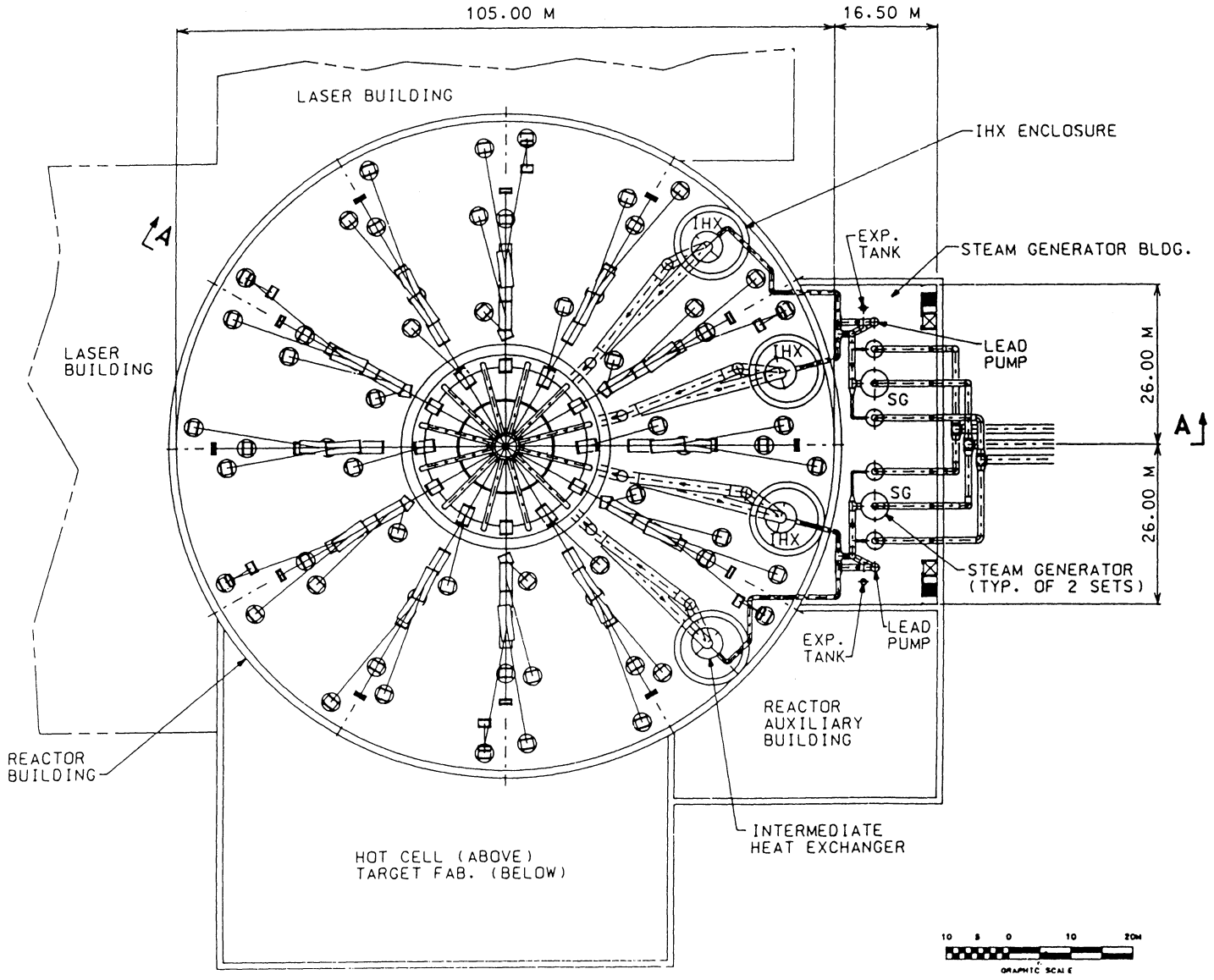

Fig. 3.4. Plan view of the SOMBRERO reactor and steam generator buildings.

replacement. In addition to the neutron dumps, the reactor building floor shields optics and equipment in the beam handling area.

Several unique features are incorporated in the reactor building structural concept. Since the building is required to operate in a vacuum, it is subject to an equivalent external pressure of about 0.1 MPa. For this reason, the floors and the ceilings are designed as shell structures rather than plates to reduce cost. The building has also been designed as a Seismic Category I structure and is adequately reinforced to resist buckling against external pressure.

A concept for the support of the grazing incidence and final focusing mirrors has been developed. As shown in Fig. 3.3, each mirror is separately supported. However, for structural rigidity, some of the supports are also tied together. Each support is a combination of reinforced concrete members. The supports are also configured so that the remote maintenance equipment can access the mirrors for replacement or refurbishment.

The IHXs are located within the reactor building. However, they are housed in individual cylindrical chambers. This arrangement accommodates the 0.1 MPa differential pressure (between the IHX chambers and the rest of the reactor building) and at the same time allows limited access to the IHX chambers during normal power operation. The steam generators are located in a separate building outside the reactor building.

3.4 KrF DRIVER DESIGN

3.4.1 Design Overview

There are several goals in the design of a KrF driver system for IFE: 1) high operating efficiency, 2) low capital cost, 3) technical credibility, 4) high availability / reliability, and 5) low operating costs. In this study we were to assume a tenth-of-a-kind plant with technology that could be mature in the year 2040. In creating a design, we focused on how to optimize operating efficiency.

A point design was carried out for a 3.6 MJ (on target) KrF laser. This is slightly higher than the 3.4 MJ we used as our reference design for the SOMBRERO power plant. To scale the design to the lower energy, the volume of the final amplifiers described in this section, would be reduced in proportion to the laser energy (i.e., by 5.6%). The design parameters for the 3.6 MJ point design are given in Table 3.3.

The KrF driver system consists of 1) a front-end which produces a pulse of the desired band width and temporal and spatial intensity characteristics, 2) several stages of intermediate amplification and progressive temporal/angular multiplexing, 3) final amplification by large e-beam pumped 2-pass amplifiers, and 4) demultiplexing and beam delivery to the reactor building. In the reactor building the beams are brought through a mirror system that provides neutron protection to

Table 3.3. KrF Driver and Amplifier Design Parameters

Overall Driver:	
Total Energy on Target (MJ)	3.6
Number of Beam Clusters	60
Beamlets per Cluster	100
Final Pulse Width (ns)	6
Efficiency (%)	7.5
Ultimate Amplifier:	
Final Amp Energy (kJ)	60
Ar in Kr (%)	50
Pressure (atm)	1
Initial Temperature (C)	500
Pumping (kW/cm^3)	400
Extraction Time (ns)	600
Amplifier Gain	16
Rep-Rate (Hz)	6.7
Length in Optical Direction (m)	1
Length in Flow Direction (m)	2
Length in E-beam Direction (m)	1
Flush Factor	1.3
Fluence (J/cm^2)	5
E-beam Voltage (kV)	610
Diode Current (A/cm^2)	40.6
Diode Impedance (ohms)	0.6
Inductance (nH)	23
Applied Field (kG)	6
Intrinsic Efficiency (%)	14.5

the laser stages and brings equal amounts of KrF illumination to the target from 60 uniformly-spaced directions by way of grazing incidence metal mirrors, which are the only optical element subjected to direct neutron flux. The ultimate amplifiers (UA's) in our system operate with a two-pass gain of 16, so the penultimate amplifiers (PA's) only supply ~6% of the total energy. From this, it is clear that the efficiency and the capital cost of the laser driver system are dominated by the UA's. Because of this, our design discussion at the conceptual stage focuses on consideration of

these amplifiers, how their efficiency may be optimized, and how they may most effectively be assembled into an architecture that satisfies the target requirements.

3.4.2 Key Features

We have produced a driver system design concept that is responsive to the requirements and goals listed above and has the following key features.

Direct Drive with Indirect Drive Brightness Capability. We have assumed the NRL, NIKE system approach for direct drive targets of "echelon-free ISI" in which a desired intensity profile is imaged onto the target through the laser chain, using partially coherent light. Broadband KrF emission with $\Delta\nu/\nu \sim 0.1\%$ is used to provide coherence times < 1 ps and thus allow rapid spatial averaging on the target. This approach utilizes imaging of a front end aperture through the whole amplifier chain, including angular multiplexing, to the target. It thus allows for the target beam spatial profile to change during the pulse and thereby takes advantage of the higher direct drive target gains that occur for a system that can zoom the target illumination spot as the target diameter decreases during irradiation. If new target designs favor indirect drive at a future date, we believe we could meet the requirements for indirect drive with a very similar system at similar cost. The ability of KrF driver systems to meet the brightness requirements for indirect as well as direct drive targets was described in a paper at the IAEA meeting on ICF Drivers in Osaka in 1991.[12]

E-Beam Pumping with High Efficiency. KrF laser kinetics and extraction physics have been studied in some detail since the first KrF lasing was achieved in 1975. Despite promising theoretical predictions for discharge and e-beam + discharge pumping, these approaches have not come close to the intrinsic efficiencies achieved by pure e-beam pumping(~ 14.5% for our present design parameters). Low efficiency of the e-beam itself has been an area of concern for e-beam pumped systems; however, Textron has recently published a technology for e-beams that will allow them to operate at high average power, for long durations, and at high efficiencies - constrained only by the albedo of the laser gas mixture.[13] E-beam efficiencies of $\eta_{eb} > 80\%$ are possible in the system we describe herein with 1 atm of 50% Ar + 50% Kr mixtures and titanium foils; η_{eb} approaching 90% should be possible with beryllium/aluminum foils. In these designs the e-beam is not allowed to intercept the foil support structure (i.e., the so called "hibachi" structure). The ability to achieve such "non-intercepting" operation has been experimentally demonstrated at Textron. This technology, coupled with the high voltage, cable-based pulse forming lines, a double foil system for removal of steady state waste heat, and the demonstrated high intrinsic efficiencies (14.5%) at high pump rate (400 kW/cm^3) and high specific energy (30 J/l-atm for our design projections) for e-beam pumping, leads to an attractive design.

Angular Multiplexing for Pulse Compression. Pulse shortening from the many hundreds of nanoseconds required for efficient operation of large e-beam pumped amplifiers, to the ~ 6 ns required for target irradiation may be reliably and efficiently achieved, at reasonable system cost, by the use of angular multiplexing. Angular multiplexing shortens the beam pulse by using arrays of mirrors to direct different parts of the beam through different path lengths and then recombining the beam parts. By sending the later sections of the pulse through shorter path lengths, the pulse duration can be shortened to that of each beam section (e.g., breaking the beam into 100 sections will shorten the pulse length by a factor of 100). This has been developed for the Aurora (Los Alamos) and Nike (Naval Research Lab.) systems, as well as others at Rutherford in England, at the University of Alberta in Canada, and the Electrotechnical Laboratory in Japan. In some of these systems, angular multiplexing was used in concert with Raman beam combining. We have not utilized Raman technology because we believe we can achieve adequate beam quality from our amplifiers without the added cost and complication of Raman conversion.

Final Amplifier Total Efficiency Optimization and Waste Heat Utilization. High overall efficiency of the final or Ultimate Amplifiers is the key for achieving higher the driver system efficiency. Efficiency optimization requires consideration of the product of efficiencies resulting from consideration of charging the pulse forming lines, losses due to pulse rise and fall times, intrinsic efficiency, losses due to amplified spontaneous emission (ASE), power used for magnets for guiding the e-beams, flow power, fill factor for the angular cavity, and delivery of 60 beam clusters to the target. With our base case design, the laser efficiency is 7.5%. As previously noted, waste heat from the laser is used for feedwater preheat in the power conversion cycle, and this increases the plant thermal conversion efficiency from 45 to 47%. An equivalent view of benefit of using waste heat is an effective increase in the laser efficiency from 7.5% to about 9.5%.

3.4.3 Final Amplifier Design

We conclude that a good compromise can be achieved with a cavity of about 60 kJ capability (energy on target) with dimensions of 1 m × 2 m × 1 m for the e-beam direction, flow direction, and optical direction, respectively. Thus, the amplifier cavity window and mirror are each 1 m × 2 m (double pass), the e-beam area is 2 m × 1 m on each side (2-sided pumping), and the flow cross section area is 1 m × 1 m. The nominal amplifier specifications are given in Table 3.3.

Key elements of our technology choices include 1) the use of cable based pulse forming lines for high power flow capability (kW/cm^2), low cost, ease of maintenance, and flexibility in architecture, 2) use of a new, non-closing plasma cathode technology that allows the realization of non-intercepting e-beam design and, thus, albedo limited transport efficiency for e-beam power into the gas, 3) low inductance e-beam design using a race track bushing for low rise/fall times,

4) flow and acoustics design evolved from the DoD repped laser technology development of recent years, and 5) superconducting magnetic coil systems for the 6 kG applied fields required for e-beam guidance.

The amplifier pulse power system consists, in sequence to the e-beam, of a DC power supply, a modulator and energy storage system, switches, parallel pulse transformers, and a 1.25 MV charging line used to charge a set of parallel wired, paper-oil cables of the sort used currently for high voltage power transmission. The cables are ~30 cm diameter and ~60 m long (determined by the 600 ns pulse length desired and the dielectric constant of the oil/paper insulation). A laser-triggered rail gap output switch is used to transfer the energy from the set of cables to the e-beam diode, which has a 1 m × 2 m cathode. The use of parallel cables for the pulse forming line, as compared to water lines in single pulse test facilities, is an approach pioneered for use in high energy rep-rate lasers for DoD applications in recent years. The cables are a well-developed technology, have relatively low capital cost, are maintenance free, and because they are flexible, allow many possibilities in system architectures.

The flow system for one of the laser cavities requires a blower to move the gas at velocity of about 20 m/s and a heat exchanger to remove the waste heat (only ~12% of energy deposited in the gas comes out as photons; the rest goes to waste heat). There are also large volumes of acoustic suppression material to damp the ~2 atm pressure jump that occurs from the deposited energy (~300 J/liter). In addition, there are flow mixers and thermal equalizers associated with reconditioning the flow between pulses to achieve the low values of RMS density perturbations consistent with maintaining good beam quality in the amplified laser beam. A nominal design consistent with these requirements is shown in Fig. 3.5. From this, we see that a 2 m flow length cavity has given rise to a 30-m-long flow loop section. The required flow loop volume is dominated by the need to achieve acoustic suppression of the deposited energy, which is proportional to the energy required on target divided by laser efficiency. Minimizing flow loop volume is directly related to optimizing laser system efficiency.

We considered a number of ways of configuring the laser cavities and settled on the arrangement shown in Fig. 3.6. Fifteen of these flow loops, each with four cavities, will supply the nominal requirements of 3.6 MJ on target. We include sixteen flow loops in the architecture, which provides four spare amplifier cavities.

The cavities in Fig. 3.6 operate as two pass amplifiers. This figure shows a grouping of four mirrors at the center of the flow loop. There is one mirror for each cavity, each set at a 45° angle to the line of sight to its cavity window. The dimensions of each mirror are 1.4 × 2 m (1 × 2 m projected area at 45°), matching the beam dimensions at the cavity mirror. The individual beams (each 6 ns long) are largest at the cavity mirrors and decrease as they go to the feed arrays. The bundles of beams from/to the feed array require approximately constant cross sectional area.

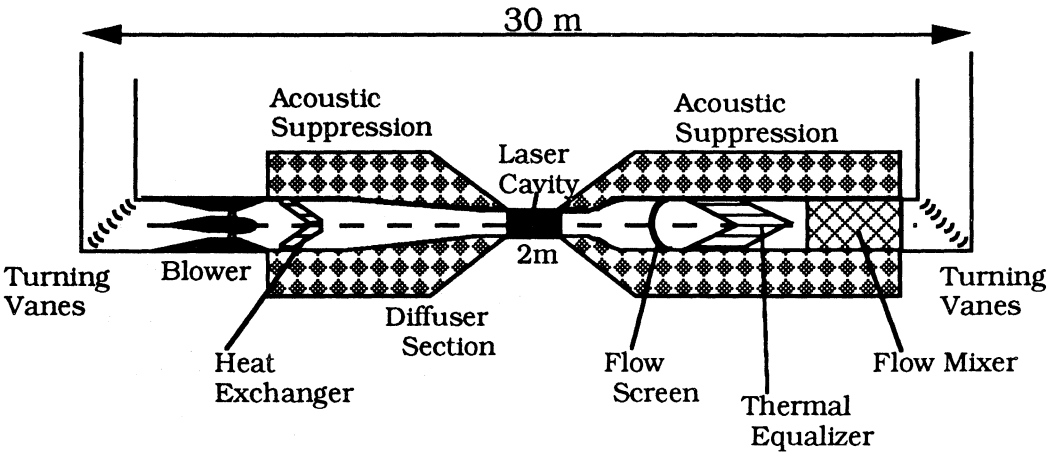

Fig. 3.5. Flow system for 60 kJ amplifier cavity (flow is from right to left).

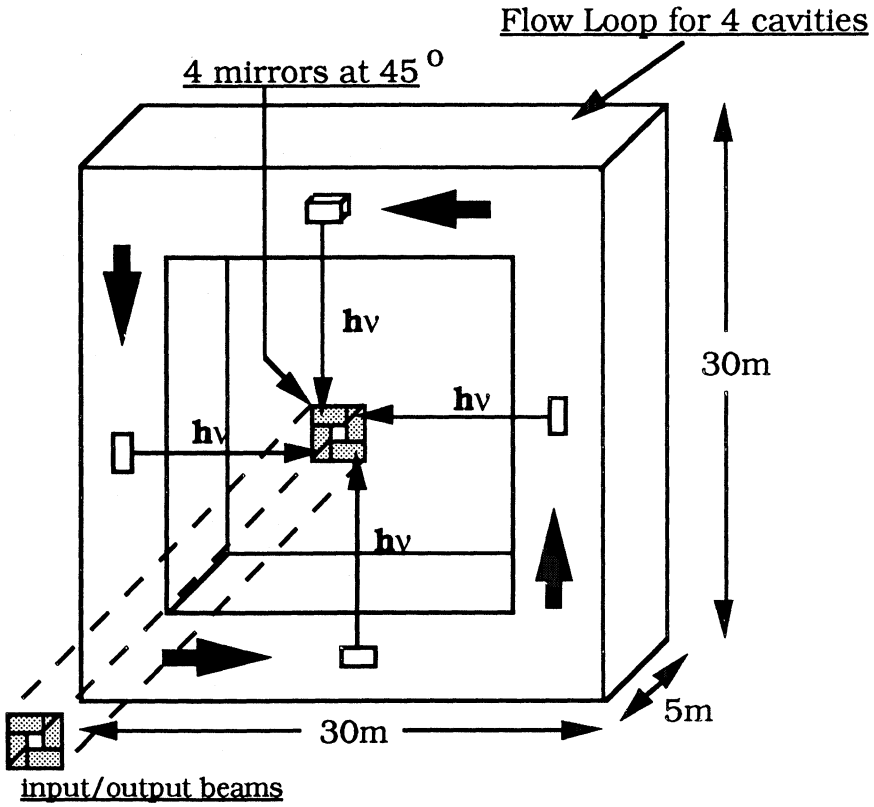

Fig. 3.6. Flow loop with four 60 kJ amplifier cavities.

Since the beam paths from the large amplifiers are in vacuum, there is an advantage in packing them together as they turn 90° to transmit from/to the feed arrays.

3.4.4 System Architecture

Our design is shown in Fig. 3.7. The total system is split into two equal parts located on the north and west sides, respectively (assume north at the top of the page). On the north side, we label the input/output array for the thirty-two 60 kJ amplifier cavities housed in eight flow loops.

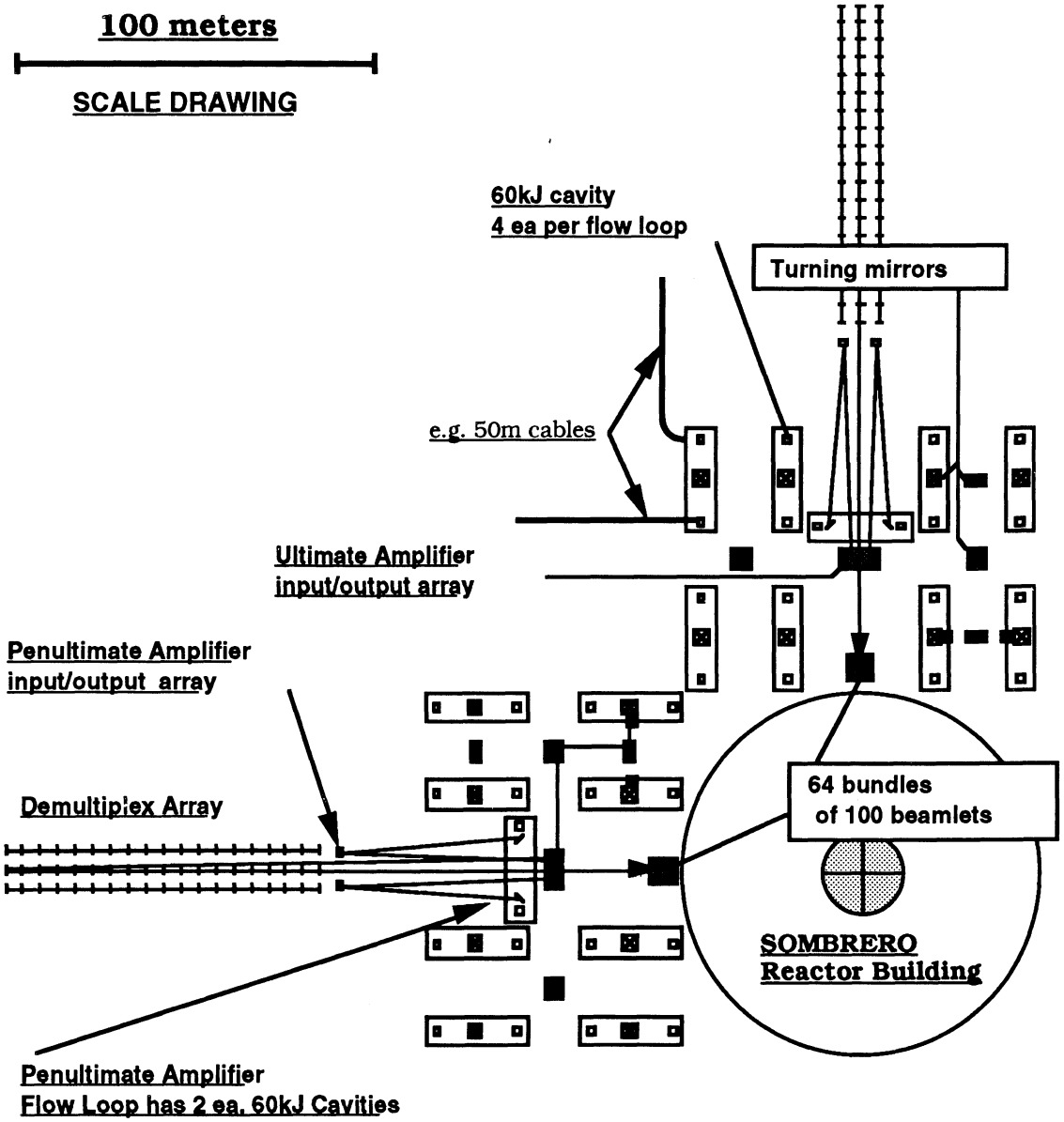

Fig. 3.7. Architecture for Ultimate and Penultimate amplifiers.

On the west side, we show a representative optical path of a single 6 ns beam leaving its 2×4 cm feed mirror, going north to a 45° turning flat, going east to the next 45° turning flat, then going north to the turning flat in the center of the flow loop, shown in Fig. 3.6, and then going into the appropriate one of the four 60 kJ cavities of this flow loop. One of these 6 ns pulses gets amplified to energy ~60 kJ/100 = 600 J since we have multiplexed the 600 ns amplifiers to one hundred 6 ns beamlets. Thus, after a double pass transit of the amplifier the beamlet follows an angularly offset path back to the input/array where it is picked up on an 8×16 cm mirror which recollimates it and sends it west to the demultiplex array. The demultiplex array provides a designed time delay and then sends the beam on to the beam handling area under the SOMBRERO building.

The total number of 6 ns beamlets is $64 \times 100 = 6400$. 6000 of these are active at any time and are distributed into 60 directions onto the target. The directions are sorted in the beam handling area under the SOMBRERO building. If the beams go the most direct route possible, there are different path lengths to the target for each of the 60 directions. Appropriate time delays may be introduced via optical "trombones" in this area and/or by use of the demultiplex array trombones. Use of the extra four laser cavities, when needed, will require that they are able to supply any of the 60 directions, which will call for special trombones and mirror insertion possibilities in the design.

3.4.5 Conclusions

We have developed a KrF laser driver system design for power plant operation that has a 7.5% overall efficiency. We achieve this by having a carefully optimized overall laser system, by using high pump rate kinetics (400 kW/cm^3) to achieve high intrinsic efficiencies (14.5%), by designing a low inductance diode structure, by using a break through gas/foil albedo limited, non-closing, non-intercepting e-beam, and by operating at high Joules/liter allowing efficient waste heat utilization. Our 60 kJ nominal size amplifier cavities give optimum efficiency and give an easy development size (the same cavity volume as the Large Aperture Module (LAM) of the Los Alamos Aurora system).

Finally, we believe our approach represents the best in low risk evolution from demonstrated technology. As in Aurora, we use e-beam pumping and angular multiplexing for pulse compression; as in Nike, we use Integrated Spatial Incoherence for smooth beam profiles in direct drive; and as in EMRLD, we use DoD-developed technology for repped excimer lasers of excellent beam quality.

4.0 TARGET SYSTEMS

4.1 TARGET PRODUCTION

4.1.1 Overview of the Reference Design

The baseline design of the target production facility contains a deuterium-tritium (DT) handling and storage facility, a fuel container (capsule) production facility, a system for filling the capsules with DT fuel, a measurement system for quality assurance (QA) purposes, and a target storage and delivery section. Figure 4.1 is a block diagram of the IFE reactor target production facility showing the major production steps.

The facility has several important features. The production equipment and overall building area are quite compact. This is largely the result of using production techniques that minimize the production time per target and thus the inventory of targets being handled at any one time. The compact design also helps minimize target production costs. Operational safety and the minimization of total tritium inventory have been considered to be critical aspects of the facility design. The tritium inventory is minimized by 1) using rapid production techniques and 2) reducing the inventory of filled targets in storage. The inventory of filled targets can be small because the system is very reliable. As indicated in Fig. 4.1, the proposed production facility is 100% redundant in order to give high reliability. Under normal conditions, each production line operates at half of its possible production rate. If a component on one line fails or requires repair, the other line is brought to full production capacity. To further enhance the safety characteristics of the production facility, the production stages and components are compartmentalized to reduce the consequences of a tritium leak in any one part of the system.

In order to produce targets economically, the production facility must be operated as a completely automated factory, not as a research facility. We assume that all processes to be employed in producing the capsules, filling the capsules with fuel, adding sabots as target carriers, and handling and manipulating targets will have been developed, tried, tested, integrated and demonstrated in a pilot plant, and perfected before use in an IFE power plant. One of the major implications of this assumption is that complete characterization of the individual targets is not required. Only an occasional measurement will be made to ensure the several fabrication processes are operating as they should.

The design is based on the production of direct drive targets as used in the SOMBRERO reactor. Production steps for indirect drive targets would be the same, except for the final step of loading the capsule into a hohlraum. Depending on its characteristics, the hohlraum could possibly serve as the sabot for the indirect drive target, thus eliminating the sabot loading step. From the

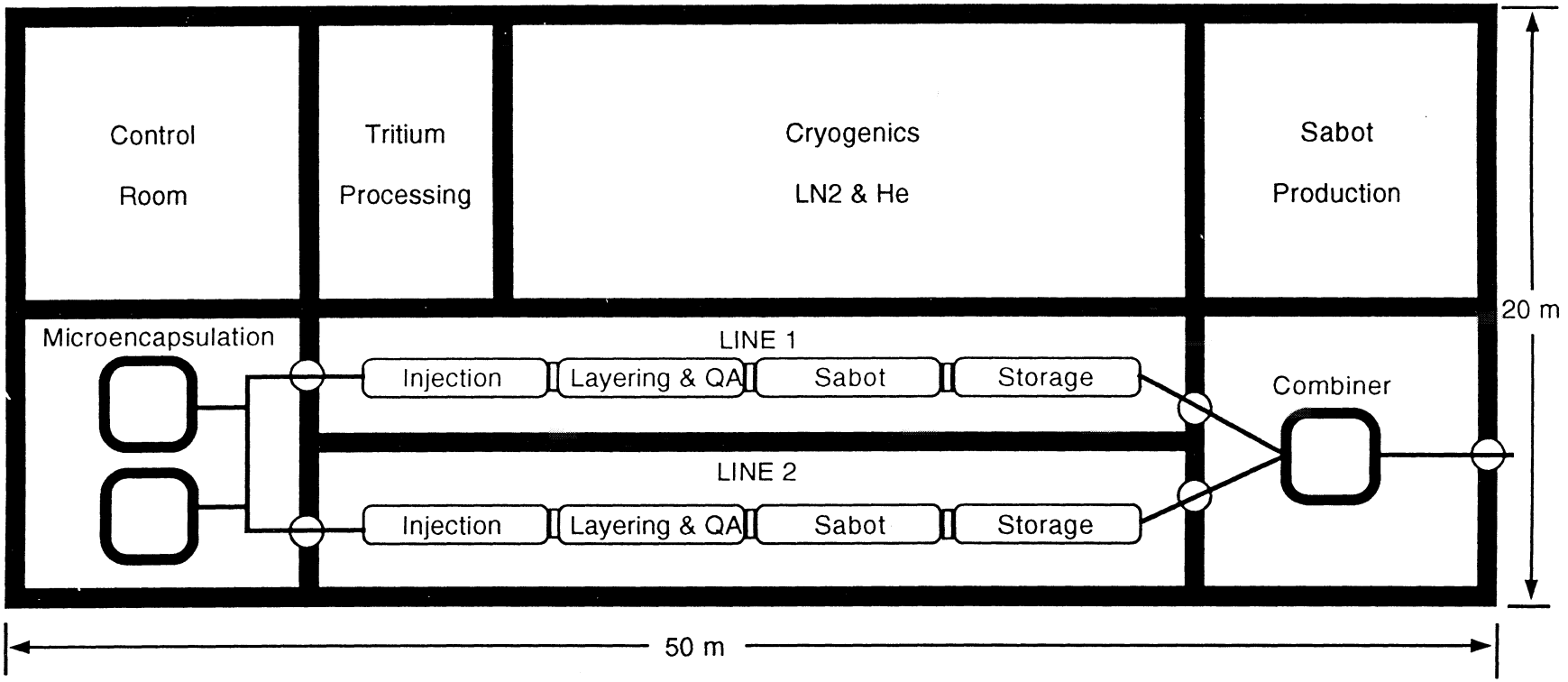

Fig. 4.1. Layout of baseline target production facility.

various options for each of the production steps, we have chosen a reference design approach listed in Table 4.1. The choices were made after considerations of several options for each of the elements of the target production facility. The options and the reasons for the choices are discussed in Chapter 4 of Volume 2.

Table 4.1. Baseline Target Production Techniques

Production Step	Chosen Technique
Capsule Production	Drop Generator / Microencapsulation
Fuel Fill	Injection Fill Techniques
DT Layer Formation	Freeze - Laser Pulse Vaporization - Refreeze

4.1.2 Capsule Production

Several techniques can be used to produce the hollow, spherical, thin wall capsules necessary for the IFE targets. The option selected for capsule production in the base case is the combination of drop generators to produce uniform liquid drops of water layered with a solution of an appropriate polymer. This has been called the controlled microencapsulation technique. It combines the advantages of the drop generator technique, which produces droplets with a fractional standard deviation in diameter of better than 10^{-5}, and the microencapsulation technique, which delivers shells which are round and have uniform wall thicknesses. A drop generator is used to produce uniform drops of polystyrene or other suitable polymer. The drops are injected directly into a liquid where they are treated to form shells as in the microencapsulation technique. Thus, shells will have uniform mass, diameter, wall thickness, and shape like those produced by the shake-type microencapsulation technique.

4.1.3 Fuel Filling

Several techniques were considered for the fuel fill step in target production. Because of the use of radioactive tritium, two major considerations were tritium inventory and safety for operating personnel.

A new and undeveloped method, called injection fill, has been selected for the DT fuel filling process because the presently available method of diffusion fill was judged to be unattractive. The basic approach to the injection fill technique is as follows:

1) A very small hollow fiber or needle is inserted through the wall of a capsule,
2) Liquid DT flows through the needle into the capsule,
3) The needle is removed from the capsule wall, and

4) The wall smoothed to a quality sufficiently high for use as an IFE target.

A hollow optical fiber could be used as the transport tube for the liquid DT fuel. The wall of the fiber forms an optical waveguide for a laser pulse that softens the wall of the capsule allowing the tip of the hollow fiber to easily penetrate the capsule. The outside surface of the fiber can be coated with a material which does not "wet" the capsule wall material. Thus, when the fiber is inserted through the wall, the wall material does not become attached to the fiber, and the wall is not severely damaged. When the fiber is removed, none of the wall material is removed by the fiber. As the end of the fiber leaves the wall, a pulse of laser light can be used via the fiber wall to heat the material around the hole. This will allow the material around the hole to flow back into the hole to repair any irregularities left by the fiber.

A large number of capsules can be filled simultaneously by using a manifold of the hollow fibers which are inserted into an equal number of capsules carried by a tray with an array of holes or cups similar to an "egg crate." The entire injection process will be carried out at cryogenic temperatures as shown in Fig. 4.2. Filling the capsules at cryogenic temperatures will ensure that there will be no disruption of the capsules because of excessive internal pressure of the fuel.

4.1.4 Developing a Uniform Fuel Layer

Some of the most stringent requirements imposed on IFE targets are on their geometry (i.e., the limits of surface roughness, wall thickness variations, concentricity of inner and outer surfaces, and volumetric uniformity of the capsule materials). The limits are particularly stringent when applied to the fuel layer inside the capsule. The fuel layer is required to be the correct thickness (i.e., correct quantity of fuel), and uniformity. If the capsule is filled with fuel in either liquid or gaseous form, in a subsequent step the fuel must be frozen into a uniform layer on the inner surface of the capsule.

Several techniques have been developed to cause the original freezing process to produce a uniform layer or to remelt and/or vaporize the fuel and implement a refreeze process leading to a very uniform layer. For our reference design, we combine the use of gas jets to levitate the capsule with a pulsed laser for rapid heating and refreezing. This technique has been demonstrated experimentally at small scale with thin fuel layers.[14] We proposed that this could be the last step just prior to insertion into the sabot and transport to the chamber. We also note that simultaneous interferometric monitoring would be possible during the layer step.

4.1.5 Capsule Handling and Transport

After they are formed, the capsules will be handled and transported in egg-crate type trays holding approximately 2000 capsules in each tray. The construction of the trays will permit handling by conveyers, robots, and other automated equipment needed to move the filled trays

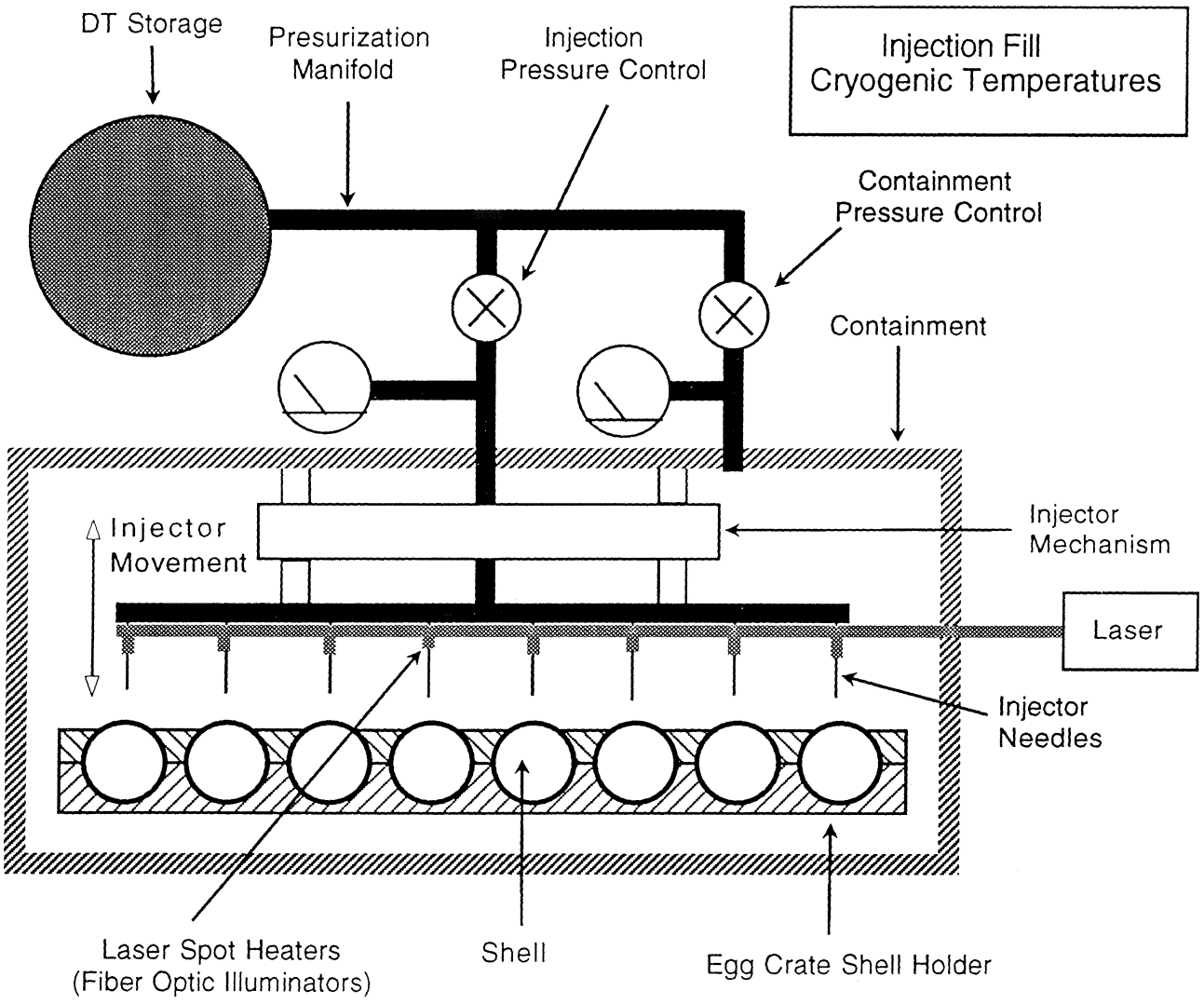

Fig. 4.2 Schematic of cryogenic injection fill system.

through the various stages of the target fabrication process. The trays will also permit automated stacking for storage and retrieval of the finished targets. To deliver targets one-at-a-time to the reactor, the trays must be unloaded and each target inserted into a sabot. The sabot is used to protect the target during transport from the production facility to the target injector and during acceleration by the injector.

4.1.6 Quality Assurance

Because the target fabrication processes must be completely industrialized by the time an IFE reactor power generation plant is built, there is no need to do a detailed characterization of each target. It will only be necessary to statistically monitor the various processes to ensure that the processes are not degrading with time. A laser interferometer will be used to generate real-time interferograms or holograms, which will be read by a high speed camera (e.g., a CCD array camera) and compared by a computer with a hard-wired, built-in pattern to determine if a given target matches the reference pattern within some predetermined limits. If differences exceed the chosen limits of size, wall and/or layer thickness, uniformity of wall, sphericity, or other parameters, alarms can alert operating personnel to potential problems.

4.1.7 Target Protection by Sabots

During the process of acceleration and transport to the outer wall of the reactor chamber, the targets will be protected by a solid sabot. The sabot will be ejected prior to entering the chamber. The sabot material will be recycled and would not add to the gas loads and contaminants dumped into the chamber at each shot. It is also advantageous to remove the sabot prior to entry into the chamber in order to keep the sabot material out of the high radiation environment.

4.1.8 Target Storage

With two production lines, each operating at half capacity, it should not be necessary to store more than 6000 finished targets in each line for a total of 12,000 targets (~30 g of tritium). This would provide for 1/2 hour of reactor operation in the event of a failure of one production line. The probability is high that the remaining line could be brought to full-up capacity in the half-hour provided by the stored targets. Because the target production processes will have been tested and perfected, reliability should be very high by the time an operating target facility is constructed.

4.1.9 Tritium Inventory

The tritium inventory of the entire target production facility can be determined within the bounds of the assumptions made for target storage, target transport during fabrication, fill process tritium requirements, and tritium in pipes leading to the fill stations. Table 4.2 provides a

Table 4.2. Total Tritium Inventory

Process Step	Inventory (g)
Injection Step	210
Layering and Q/A Steps	10
Sabot Loading	10
Storage of Complete Targets	29
Transport Chain to Chamber	1
Piping and Purge Lines	40
Total Tritium Inventory	300

tabulation of the tritium inventory for the IFE fusion reactor target production facility. The estimated total tritium inventory for the target production facility is about 300 g.

4.1.10 Production Facility Building

We propose that the capsule production, fill system, transport, storage, sabot production and loading, and other target handling functions will all be accomplished in clean (10-100 class), enclosed "boxes." Thus, it will not be necessary to build the target production facility building to clean room specifications. It will be sufficient to have the entire facility at 10,000 to 100,000 class cleanliness. The entire apparatus in which targets are filled, transported, manipulated, and stored will be constructed for total containment of the tritium so the building itself need not be more costly than ordinary construction.

4.1.11 Summary

The follow points summarize the features of the target production facility design:

- Our design approach will lead to high reliability due to 100% redundancy of process lines.
- The tritium inventory is minimized by using fill and layering techniques that can be completed in seconds instead of hours.
- A small capsule storage inventory is judged to be acceptable because of the redundancy and high reliability.
- The required building is compact, which should lead to acceptably low cost.
- Much of the technology is unproven and requires development.
- The payoff in pursuing these innovative target production approaches is very high in terms of reducing the tritium inventory and the size and cost of production equipment and buildings.

4.2 TARGET INJECTION, TRACKING, AND POINTING

4.2.1 Introduction

In order for the driver to ignite the target and produce the gain necessary for an IFE reactor, the final driver beams must all be centered on the target and hit the target simultaneously. Three separate systems must work together to accomplish this:

1) Target delivery to the correct location in the chamber must be as consistent and accurate as possible.
2) A tracking system must be able to detect small variations in the placement of individual targets in time to correct the beam pointing.
3) An active beam alignment system must be able to quickly and accurately point the beams to each target's final location.

4.2.2 Injector System

Figure 4.3 is a schematic of the baseline target injection and tracking system that uses a gas gun for target acceleration. After leaving the acceleration section, the target travels a constant velocity to the center of the chamber. A removable sabot is used to protect the target during acceleration. The target is given an angular velocity during acceleration, so the sabot will be separated into two pieces by centrifugal force after acceleration. The distance from the exit of the acceleration section to the center of the chamber is divided into three segments: the sabot removal length, the tracking length, and the radius to the outer edge of the chamber. Design parameters for the injection system are given in Table 4.3.

Table 4.3. Baseline Target Injection Parameters

Acceleration (g)	130
Accelerator Length (m)	9
Final Injection Velocity (m/s)	151
Time in Accelerator (m)	119
Sabot Removal Length (m)	2.5
Time for Sabot Removal (m)	17
Rotational Velocity for Sabot Removal (RPM)	570
Time for Tracking (ms)	50
Time in Chamber (ms)	50
Total Time from Target Firing to Ignition (ms)	235
Time Allowed for Coarse Corrections (ms)	100
Time Allowed for Fine Corrections (ms)	50

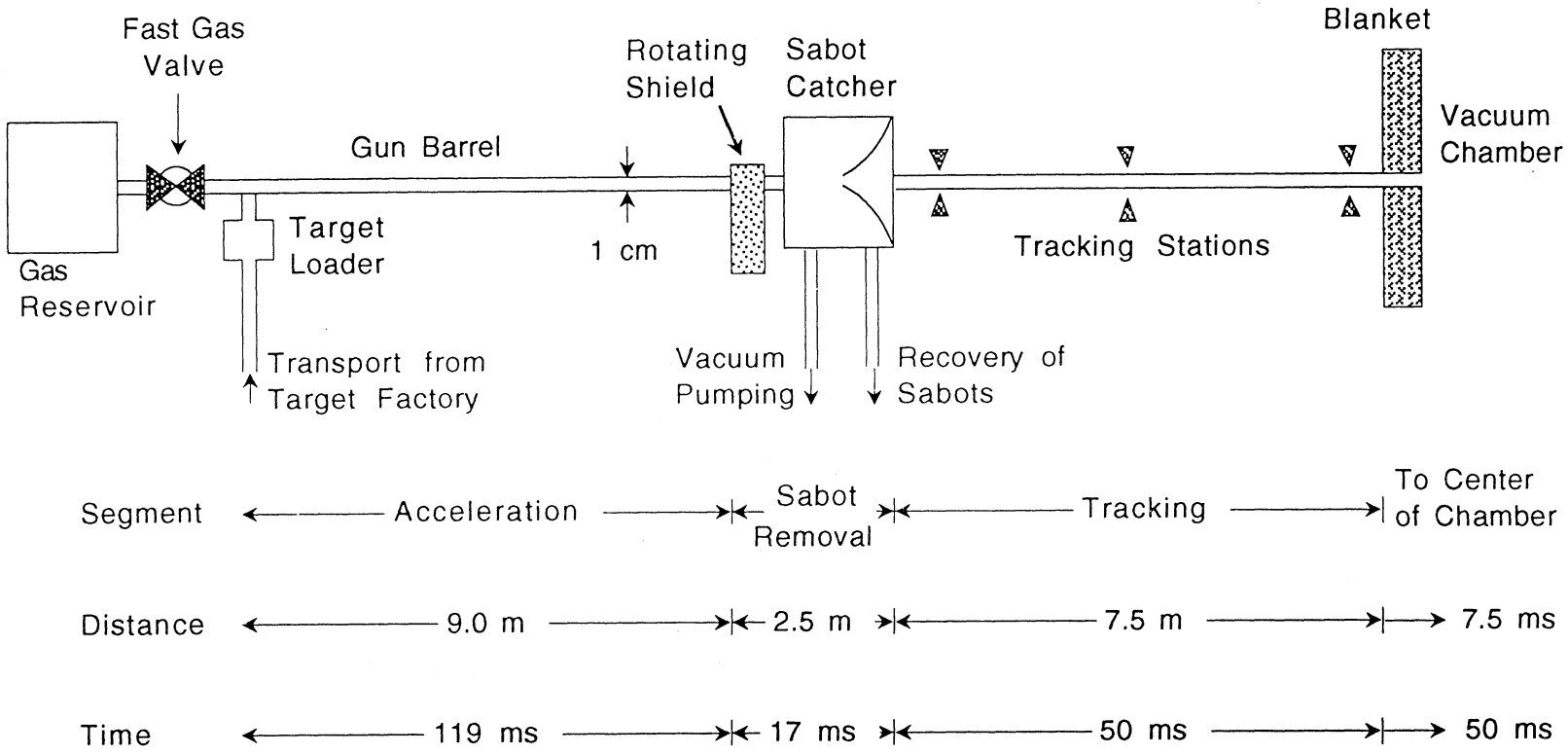

Fig. 4.3. Schematic of the reference design for the target injection and tracking system.

The light gas gun was chosen as our base injector because of its relative technical maturity, low risk, and its ability to give accurate target placement at required repetition rates. A light gas gun uses a high pressure hydrogen, deuterium, or helium gas to accelerate the frozen pellets of fuel through a tube or barrel. The velocity of the pellet is limited by the driving gas parameters and the projectile size and mass. Rifling of the barrel can be used to provide the required spin rate for sabot removal. A gas gun will require that the sabot form a tight seal with the barrel of the injector. Acceleration limits on targets, heating of the sabot, barrel wear, and loading, recovery and refilling of sabots are critical issues which must be addressed.

4.2.3 Tracking System

Our base tracker consists of a laser Doppler velocimeter followed by a series of crossed light axis position and time detectors as shown in Fig. 4.4. The assumed pointing accuracy for the gas gun (10 microradians) and the expected shot-to-shot velocity variation (± 3 %) combine to set limits on tracker field of view. The tracker design must be sized to accommodate these variations in gun performance.

A possible one-dimensional tracker for use in an X-Y position detector could consist of a Ga-As laser diode beam which is expanded to approximate 5 cm in diameter and then be refocused on a silicon diode array of 40×100 elements for Y direction and 20×100 for the X direction to accommodate the initial pointing inaccuracy. Each array will be scanned at 10 MHz to assure that the pellet is repeatedly sampled as it passes through the beam. This approach allows at least ten totally independent measurements of the target position at each station (two pair of cross-axis laser and detector rings), providing noise reduction and accuracy improvement in each axis.

Velocity will be estimated at each station. Because of the limited distances between measurements, the accuracy of the velocity measurement can be greatly improved by using at least four sets of stations. These stations will give independent velocity measurements separated by 10 ms, and Kalman filter prediction algorithms will be developed to estimate the target trajectory to the intercept point. The first estimate of intercept location and time will be available 100 ms before intercept, requiring that the beam pointing element have a bandwidth of > 100 Hz. This will allow at least ten time constants for the system to accurately settle and match the intercept location.

4.2.4 Beam Pointing

Laser Beam Pointing. If the pointing system has most of the 100 ms available for settling, the requirements on fast steering mirrors are minimized. Fast steering mirrors with settling times well below 100 ms have been built as part of SDIO programs.[15] One example is the cooled fast steering mirror system with a 600 Hz bandwidth used by United Technology

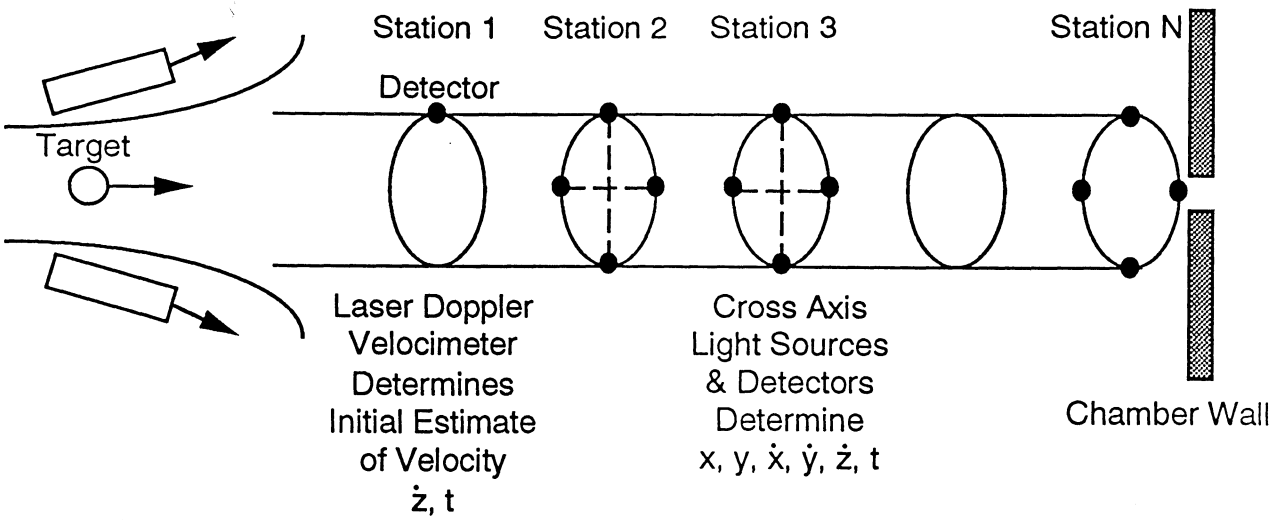

Fig. 4.4. Tracking system using multiple tracking stations.

Optical Systems for the FEL program, but these highly accurate cooled mirror systems are expensive and complex. The uncooled 10 cm size, 100 Hz bandwidth mirrors needed by this design are less complicated and have lower demands; they should not be a driving cost item in the laser system.

Heavy-Ion Beam Pointing. Pointing the HIB requires measuring the location an direction of the beam and referencing it to the tracking system. The first problem is to measure the beam location. While it is unlikely that a beam measurement on a single shot could be used to focus that same shot, beam sensing can be used for shot-to-shot corrections of a driver. Beam bug techniques developed at LLNL and the beam position monitor developed at LANL for the SDIO Neutral Particle Beam (NPB) program could be used to provide the basis for a beam-sensing design.

Pointing of the heavy-ion beams will be done by a pair of crossed dipole steering magnets. These steering magnets could consist of coils inside the final focusing quadrupole magnets. Preliminary calculations give steering bandwidths on the order of 100 kHz which far exceeds the required response time for an IFE pointing system. Critical issues which must be investigated are the linearity, repeatability, and accuracy of the steering magnets.

4.2.5 Summary

Target systems for target injection, target tracking, and beam pointing all require significant development work. Fortunately, many of the required elements have been demonstrated by directed energy weapon research programs. We have presented a conceptual design for an integrated injection, tracking, and pointing system using existing technology which should be able to meet all the requirements of an IFE reactor after a significant design development effort.

4.3 TARGET HEATING DURING INJECTION

4.3.1 Introduction

The targets contain cryogenic fuel, which must not liquefy or vaporize prior to implosion. The targets also have very precise dimensions in their non-fuel shells, which must be maintained prior to irradiation by the driver beams. The required vapor pressure inside the central void of the target is a strong function of the fuel temperature and must also be maintained at a prescribed level. A preliminary assessment was made of the effects of heating due to radiation from the target chamber walls and due to convective heat transfer from the target chamber gas.

4.3.1 Heat Loads

We have considered two types of heat loads on the surfaces of both target types; convective heat transfer from the chamber gas to the target and radiative heat transfer from the target chamber walls. The gas conditions are very different in the two reactor designs. The target velocity for both reactor concepts are ~150 m/s. The approximate heat loads for the two target are given in Table 4.4.

Table 4.4. Target Heat Loads

	SOMBRERO	Osiris
Wall Temperature (K)	1758	923
Gas Temperature (K)	1758	923
Gas Density (cm^{-3})	3.55×10^{16}	3.55×10^{12}
Gas Species	Xenon	Flibe
Conductive Heat Load (W/cm^2)	4.2	6×10^{-5}
Radiative Heat Load (W/cm^2)	54.2	4.1
Total Heat Load (W/cm^2)	58.4	4.1

4.3.3 PELLET Computer Code

The PELLET computer code was developed at the University of Wisconsin to simulate the heating of ICF targets by the target chamber environment. PELLET uses information on the target geometry and the surface heat load to calculate the temperature at every position in the target as a function of time. Temperature dependent material properties were used in the calculations.

4.3.4 Results

The results of the PELLET code calculations are summarized in Table 4.5. The peak temperatures in the different parts of the target are given.

Since the Osiris target must travel ~ 5 m through the chamber and is injected at a velocity of 150 m/s, ~33 ms will be required for the target to reach the ignition point. At the estimated heat load of 4 W/cm^2, the fuel would only reach about 8 K by this time.

The targets for SOMBRERO must travel 6.5 m through the chamber before it is imploded and if the targets travel at 150 m/s, the target surface is heated for 43 ms. At 58 W/cm^2, we estimate the outer fuel temperatures to be ~17 K. This is still below the triple-point, but there is only a 4 K margin for error. While the fuel remains below the triple point, the outer surface temperature of the polystyrene capsule is ~700 K. Since this is well above the melting point of polystyrene, it will be necessary to protect the capsule during transit through the chamber. One possibility is to keep the capsule in the sabot for most of the transit time. Another option is to freeze a thin layer of inert gas (e.g., xenon) on the outer surface of the capsule. The frozen gas would act as a sacrificial heat sink and evaporate as the capsule transits the chamber. This could reduce the time that the bare capsule is exposed to the hot chamber to a few milliseconds. Clearly, this is an area that requires further investigation.

Table 4.5. Peak Temperatures in Different Parts of Target

	Osiris	SOMBRERO
Time (ms)	33	43
Hohlraum	22	N/A
Capsule	22	700
DT Fuel	8	17

5.0 ENVIRONMENTAL AND SAFETY ASSESSMENT

5.1 INTRODUCTION

A strong emphasis has been given to the environment and safety issues in both the SOMBRERO and Osiris reactor designs. Carbon/carbon composite has been used as the chamber material to avoid a high level of induced radioactivity in both reactor structures. Similarly, the use of Li_2O in SOMBRERO and Flibe in Osiris as coolant and breeder materials eliminates the hazard posed by the energy-producing chemical reactions usually associated with the use of lithium and, hence, reduces the risk of mobilizing the radioactive inventory present in both reactors.

A detailed activation analysis was performed in order to calculate all possible radioactive inventories for each of the two reactor designs. Results of the radioactivity calculations were used to evaluate the following:

1) The biological dose rate at different locations inside the reactor building following shutdown to assess the feasibility of hands-on maintenance
2) The radwaste classification for each region of the reactor
3) The maximum public dose from routine operational effluents
4) The off-site doses from accidental release of the radioactive inventories present in the reactor building, target factory, and fuel reprocessing facility.

5.2 SAFETY DESIGN GOALS

The main safety goals for both the SOMBRERO and Osiris reactor designs are:

1) Limiting the need for remote maintenance and allowing for hands-on maintenance by reducing the biological dose rate following shutdown below 2.5 mrem/hr by increasing the biological shield where it is possible.
2) Disposing the reactor structure and coolant as either Class A or Class C low-level wastes as regulated by the Nuclear Regulatory Commission's (NRC) 10CFR61 guide lines.
3) Limiting the public dose to the maximally exposed individual (MEI) from routine operational effluents to less than 5 mrem/yr.
4) Limiting the whole-body (WB) early dose during a conservative accident scenario to 25 rem, which was recommended for this study by the study guidelines. The low off-site dose will allow for the avoidance of early fatalities in case of an accidental release of radioactivity.
5) Eliminating the need for the use of N-Stamp nuclear grade components.

5.3 RESULTS

The key results of the environmental and safety assessment are summarized in Table 5.1. The SOMBRERO and Osiris reactor designs have distinct favorable safety characteristics. Because of the double wall layout used in SOMBRERO, the biological dose rate behind the steel-reinforced concrete shield is low enough to allow hands-on maintenance inside the IHX enclosures within a day after shutdown. The dose rate after shutdown behind the 3 meter biological shield of Osiris is only 0.1 mrem/hr allowing for hands-on maintenance. However, only remote maintenance is allowed in the space between the chamber and shield of both reactors. The chamber and shield of both reactor designs qualify for near surface burial as Class A low level waste. Using the NRC waste disposal limits for solid waste, both the Li_2O solid breeder and Flibe could qualify for shallow land burial as Class C and Class A low level wastes, respectively. However, Flibe has to be in solid form before such disposal can take place and the feasibility/practicality of such a process has to be determined.

Some tritium does reach the off-site environment during normal operation. The reactor system, the reactor building, the fuel reprocessing facility, and the target factory are the major sources of routine release of tritium. Assuming a barrier factor of 10^6, the doses from the atmospheric routine release of tritium from SOMBRERO and Osiris to the maximally exposed individual are 0.93 and 2.43 mrem/yr, respectively. Both values are far below the 10 mrem/yr EPA current effluent limit. The site boundary is assumed to be at 1 km from the point of release. The off-site doses caused by an accidental release of radioactivity from both reactor designs are dominated by the dose resulting from the off-normal release of tritium. During an accident, the maximum vulnerable inventory of tritium in SOMBRERO is 183 g. Most of the tritium (162 g) is contributed by the Li_2O granules. On the other hand, due to the small tritium inventory in Flibe salt (1 g), the maximum vulnerable inventory of tritium in Osiris is only 13 g. The estimated off-site whole body (WB) early dose released from SOMBRERO due to a highly unlikely sequence of simultaneous accident scenarios involving, the reactor chamber, biological shield, breeder, and tritium is 2.22 rem. This dose is below the 5 rem level where evacuation plans are needed and far below the 25 rem value recommended for this study by the oversight committee as a threshold for avoidance of early fatalities. Assuming similar accident scenarios, the Osiris design would result in a WB early dose of only 0.13 rem.

An accident analysis involving the target factory facility showed that a 100% release of the 300 g of tritium expected to be present inside the facility at any moment would result in a WB early dose at the site boundary of only 2.70 rem, which again is below the limits required for public evacuation. Finally, an accident resulting in the release of the total inventory of tritium existing in the fuel reprocessing facilities of SOMBRERO and Osiris would produce off-site doses of only 0.68 and 0.48 rem, respectively. The very low off-site dose for either reactor designs

eliminates the need for N-Stamp nuclear grade reactor components, which are only required if the dose exceeds the 25 rem limit.

Table 5.1. Comparison of Environmental and Safety Results

	Osiris	**SOMBRERO**
Maintenance of Chamber Components	Remote	Remote
Maintenance of Power Cycle Components	Hands-on	Hands-on
Chamber Radwaste Classification	A	A
Shield Radwaste Classification	A	A
Breeder Radwaste Classification	A	C
Routine T_2 Release (Ci/d)	92	93
Maximum Dose to Exposed Individual from Routine Release (mrem/y)	2.43	0.93
Total T_2 Inventory (g)		
Reactor	13	183
Fuel Processing	54	74
Target Factory	300	300
Accidental WB Early Off-Site Dose at 1 km (rem)		
Reactor	0.13	2.22
Fuel Processing	0.48	0.68
Target Factory	2.70	2.70

6.0 RELIABILITY, AVAILABILITY, AND MAINTAINABILITY ASSESSMENT

6.1 INTRODUCTION

A preliminary reliability, availability, and maintainability (RAM) assessment was performed on the SOMBRERO and Osiris reactor plants. The primary objectives were to assess the RAM aspects of the two designs and to establish availability goals for the major plant systems to aid in planning future development efforts.

6.2 AVAILABILITY ASSESSMENT

The SOMBRERO and Osiris power plant designs are not detailed enough to estimate plant availability with any confidence. The approach, therefore, was to first make a rough estimate of the availability of the plant subsystems and then to use these estimates to establish availability goals for the major plant systems that combine to the give the desired availability goal for the entire plant. The initial estimates are in essence weighting factors for allocating system availability goals.

To assess the availability, each reactor plant was partitioned into four major systems: driver, reactor, target (fabrication, injection, and tracking), and energy conversion/balance-of-plant. Each of these major systems was divided further into several functional subsystems, and an achievable availability was estimated for each subsystem. The estimated availability was determined based on existing similar systems or comparable systems taking into account expected component lifetime, equipment random failure rate, power output fractions, manufacturing process capacity factor, and in-process storage capacity.

The estimated availability values for the major SOMBRERO and Osiris systems are summarized in Table 6.1. The availability due to unplanned down-time is slightly less than 70% for both plants.

Table 6.1. Estimated Availability for Osiris and SOMBRERO Plant Systems (Due to Unplanned Events)

	Osiris	SOMBRERO
Driver Systems	0.87	0.89
Reactor Systems	0.90	0.89
Target Systems	0.92	0.90
Energy Conversion & BOP	0.96	0.96
Total	0.69	0.68

Based on the estimated subsystem availability, the overall plant availability goal was apportioned to individual subsystems according to a model described in Ref. 16. An overall plant availability goal of 75% is assumed for the IFE reactor plants so as to be comparable to other fusion reactor studies and current large electric power generating systems . To achieve this goal, the required effective operation availability is 81% after allowing for an assumed downtime of four weeks each year to account for preventive maintenance activities.

Availability allocation is apportioned for plant systems from the top down according to the reliability and maintainability characteristics of the systems in such a way as to achieve the plant availability goal. The availability apportionment indicates the optimum balance of availabilities for all systems in the plant. The allocation process serves as a means of assessing the design and defines availability improvement targets in system design refinement. These improvements include better system design, application of redundancy, changes in maintenance concepts, or combination of these options.

Using an effective operation availability goal of 81% for the IFE reactor system and the estimated system availability values in the above section, the availability goals for various SOMBRERO and Osiris plant systems are established as indicated in Table 6.2. Comparing these goals to the rough estimates given in Table 6.1 indicates that for both plants, 4-5% improvements are need for the drivers, reactors, and target systems, and a 2% improvement is required for the BOP availability in order to meet the overall plant availability goal. However, since RAM data for these systems are mostly nonexistent, or at best available from limited experimental results, these results should not be considered conclusive. More definitive assessments will require detailed designs and evaluations of the plant systems, additional data obtained from extended test periods, and eventually the integration of driver, target, reactor, and BOP systems in an experimental test facility.

Table 6.2. Allocated Availability Goals for SOMBRERO and Osiris

	Osiris	**SOMBRERO**
Driver Systems	0.94	0.93
Reactor Systems	0.94	0.95
Target Systems	0.94	0.94
Energy Conversion & BOP	0.98	0.98
Total Unplanned	0.81	0.81
Planned	0.92	0.92
Overall	0.75	0.75

6.3 MAINTAINABILITY OF THE OSIRIS PLANT

An analysis was performed on the sequence and type of activities required in order to remove and replace the Osiris vacuum cover, fabric blanket assemblies, and the maintenance of other reactor support equipment. The activities that define the classes of operation for the Osiris reactor design are as follows:

- High and Low Pressure Flibe Inlet Pipe Disconnect
- Driver Seal Flange Unbolting and Retraction
- Vacuum Chamber Cover Unfastening and Interference Removal
- Vacuum Chamber Cover and Attached Internals Removal
- Reinstallation

The Osiris reactor building size is dictated by the maintenance handling requirements for the vacuum vessel cover and reactor internals. These requirements were due to the complexity of refurbishment operations associated with these components, constraints which dictated that the cover and internals be removed as one piece. The physical size of these components and the complexity of refurbishment operations suggested that it is prudent to "replace in kind" rather than "refurbish in place." With this in mind, it became apparent that the remote handling equipment needs to have common access to both the reactor building and the hot cell/maintenance areas. To accommodate this requirement, a large movable shield wall is provided. As illustrated in Fig. 6.1, this shield wall is located between the reactor building and hot cell, and the crane bay containing all of the overhead operated remote handling equipment is open to both. The remote handling equipment is protected from neutron activation during reactor operation by extending the shield wall in place and locating the equipment at the far end of the hot-cell facility. The hot cell contains both a clean room in which to store the new replacement cover and reactor internals (thus isolating them from the old contaminated internals being removed) and a hot storage area, which is a large temporary containment that houses the old components being removed.

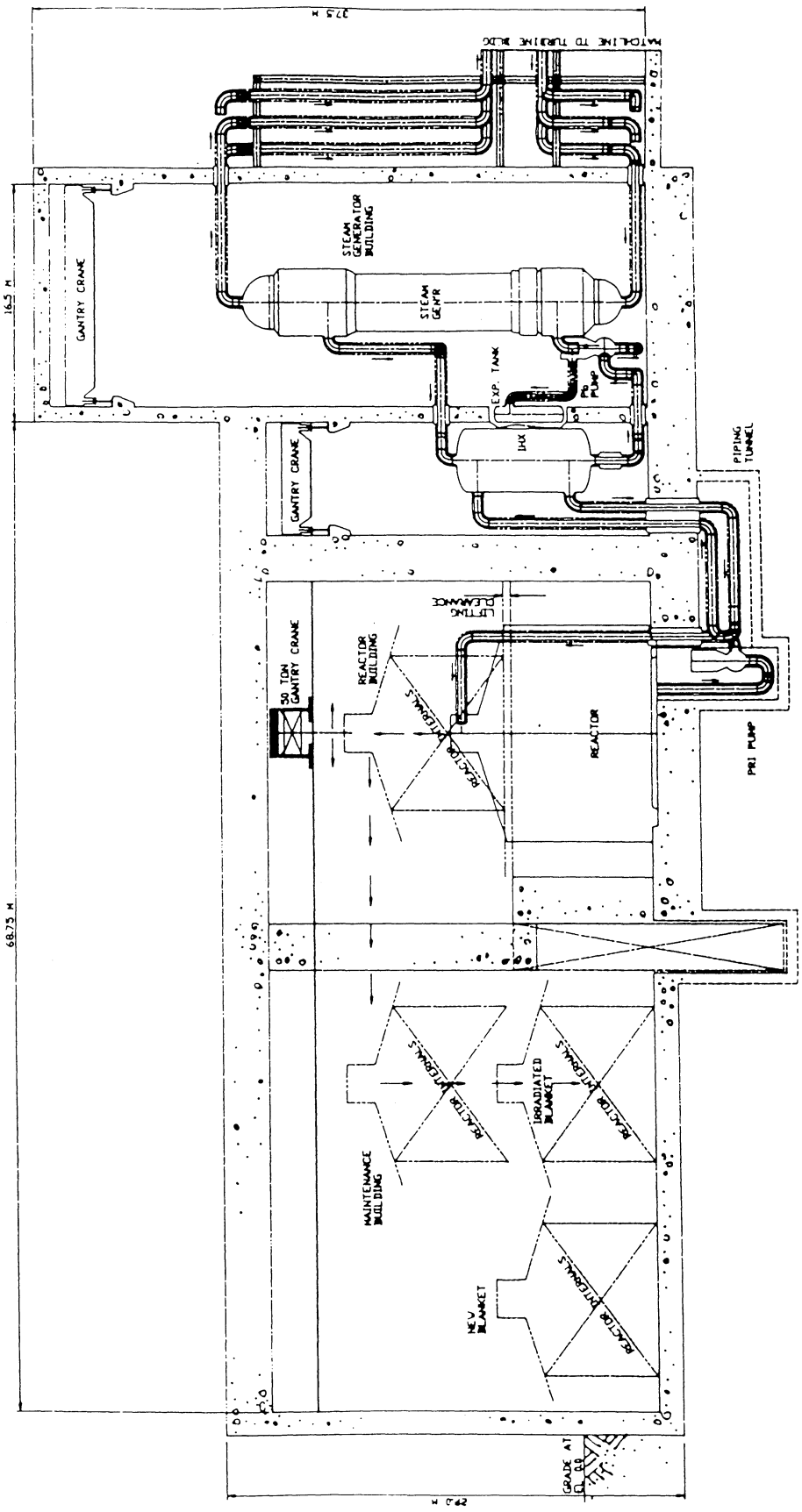

Fig. 6.1. Cross section view of Osiris maintenance procedure.

6.4 MAINTAINABILITY OF THE SOMBRERO PLANT

A methodology similar to the Osiris was used to develop an approach for remote maintenance of the SOMBRERO reactor. An analysis was performed on the sequence and type of activities required in order to remove and replace the reactor module assemblies and the optics within the reactor building. An evaluation of the activities was performed to define the classes of operations that would be conducted. In an effort to determine a baseline case for overall remote handling equipment operational envelopes and equipment and component handling sequences (for maintenance activities), the activities that would define the classes of operation for the SOMBRERO reactor design are as follows:

- Upper Plenum/Inlet Pipe Removal
- Module Removal/Replacement
- Mirror and Optics Maintenance
- IHX Maintenance
- Reactor Support Equipment Maintenance
- Beam Handling Equipment Maintenance
- Hot Cell Operations.

Due to the large physical size of reactor building (dictated by the optics requirements), an innovative approach to crane operations and rigging and handling of components was necessary. For this case, both the polar crane and annular crane make use of the National Institute for Standards and Technology (NIST) high payload automated crane concept. This concept employs a modified Stewart platform where the hook and block-and-tackle are normally located. This platform allows for very stable control of heavy offset payloads at long distances from the cable drum and trolley assembly. The most unique design feature of SOMBRERO is the remote handling equipment designed to handle the chamber modules. Each of these modules is approximately 24-m tall and 8-m deep. Due to space restrictions in the center reactor building volume, each of these modules is designed to be removed and replaced one at a time. As illustrated in Fig. 6.2, the removal sequence dictates that the module be lowered to the bottom of the inner cylindrical chamber, installed on a polar carriage assembly (which accommodates radial positioning), and tilted out of the lower access door via a transport carriage, through the annular space and into the hot cell facility. This whole evolution is analogous to current practices in fuel bundle handling systems currently in use.

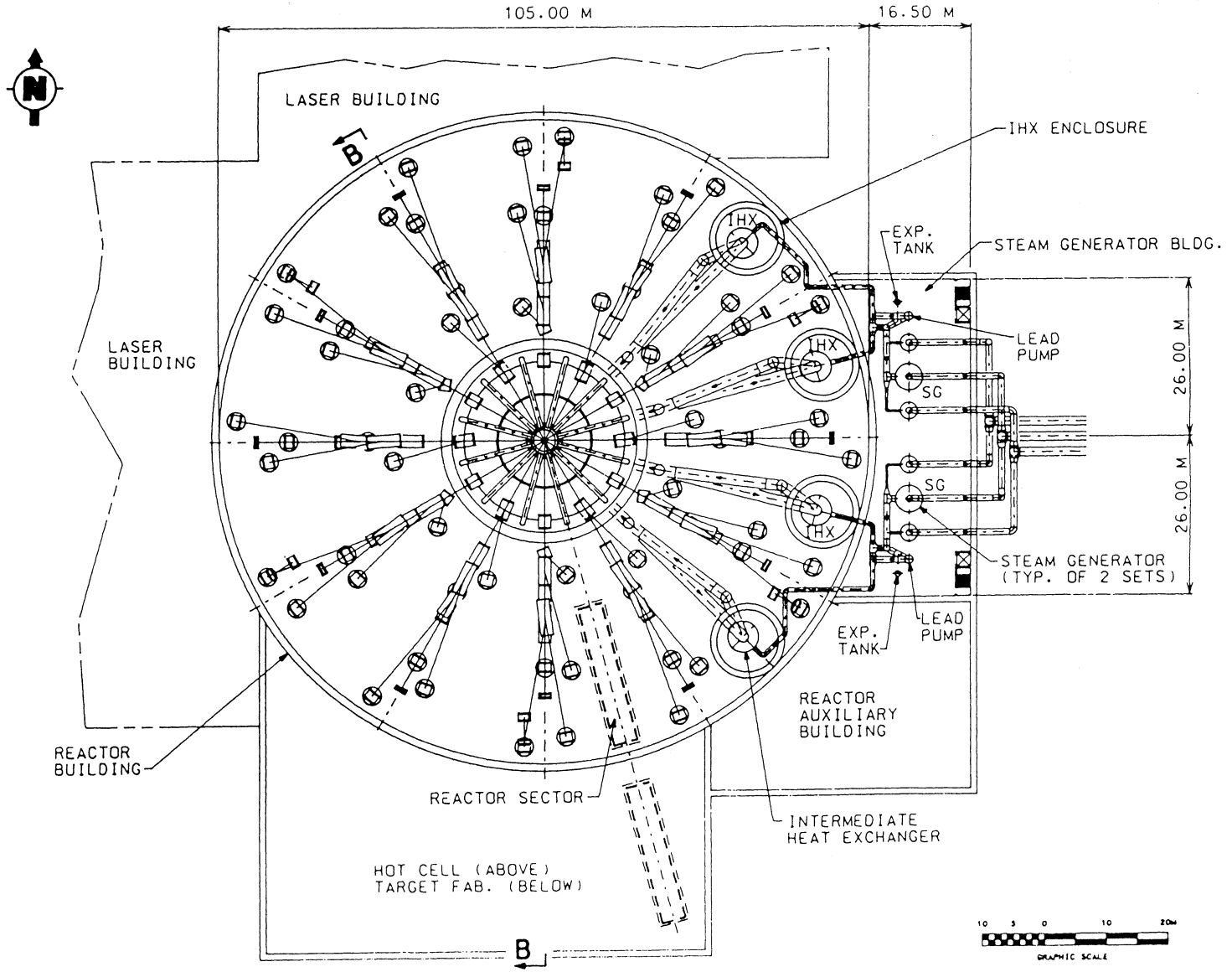

Fig. 6.2. Cross section view of SOMBRERO maintenance procedure.

7.0 TECHNOLOGY ASSESSMENTS

7.1 INTRODUCTION

Many assumptions have been made during this study about materials capabilities, component availability and performance, and cost. In Chapter 7 we attempt to put all this in perspective and assess the technical issues, development needs, and level of urgency. A semi-quantitative approach was taken with issues weighted on a scale from zero (low) to 100 (high) in increments of 25. The issues and weighting factors are given in Table 7.1.

Table 7.1. Technical Issues and Weights

Technical Immaturity	10%
Critical Technology	30%
High Development Cost	30%
Long Lead Time	20%
% Cost in Experiments	10%

Note that they are defined in terms of concerns (e.g., technical immaturity rather than maturity) so that a high score always indicates a problem. The weightings are obviously judgmental. Technical immaturity is far less important than critical technology (i.e., no alternative technologies or approaches exist) or development cost. These last two are considered the most important. Long lead time is also an issue. An example of an issue with a long lead time would be materials development. Some account is also made of the greater developmental uncertainty when many experiments are required.

The areas covered for Osiris and SOMBRERO are reactor chamber, shielding, final beam transport, coolant and ducting, IHX, steam generator, power conversion, driver, and target fabrication and injection. Other areas generic to IFE regardless of the specifics of the reactor chamber and driver include target design and innovations, systems modeling, low-activation materials, and remote maintenance.

7.2 SUMMARY OF DEVELOPMENT PRIORITIES FOR OSIRIS

Table 7.2 summarizes the results of the technology assessment for Osiris listing current technical credibility (i.e., the current state of the art) for each item, as well as development needs for reactor applications. It also shows a ranking of the development priorities for each major

subsystem. The development needs are not necessarily the inverse of technical credibility, because, in many cases, rather simple experiments can resolve major issues. The level of expense and difficulty has been included, as has the impact of the issue on reactor performance and cost.

Not surprisingly, the driver ranks first in development priority. Part of this is due to the enormous potential expense and part because of the limited development paths: RF or induction and once-through or recirculating.

The target factory ranks second because so little is known about economic, automatic fabrication of cryogenic targets. Hopefully, the ongoing research on target fabrication will help. Nevertheless, a concerted effort must be undertaken to scope out a reactor-relevant target factory in some detail.

While one might expect the reactor chamber to top the list, it is preceded by the two above partly because the development needs can probably be met with less expense, and there are many other reactor concepts to fall back on. This is not true with the driver and target factory.

Target injection and tracking doesn't rank as high as expected in development priority partly because of the relatively modest scale experiments that are required and because of related technology existing in the MFE and SDI programs.

The remaining items lie some distance down the development priority scale although there are certainly numerous design issues that must be addressed.

Table 7.2. Osiris Development Priorities

Item	Current Technical Credibility	Development Needs	Devel. Priority
Driver	Low	High	1
Target Fabrication	Low	High	2
Reactor Chamber	Low	Moderate	3
Target Injection	Moderate	Moderate	4
IHX	Moderate	Low	5
Steam Generator	Moderate	Low	6
Flibe Pumps/Ducts	High	Low	7
Shielding	High	Low	8
Reactor Building	High	Low	9
Power Conversion	High	Low	10

7.3 SUMMARY OF DEVELOPMENT PRIORITIES FOR SOMBRERO

Table 7.3 gives a summary of the technology assessment for SOMBRERO, listing technical credibility of the current state of the art for each item, as well as development needs for reactor applications. It also shows a ranking of the development priorities for each major subsystem.

As with the Osiris reactor, the driver ranks first in development priority. The key issue is cost, which translates into technical issues like material selection, fabrication techniques, and tolerances. Reliability and component lifetime are related to cost, of course, but they have been separated out here as an issue that will require considerable development. The remaining driver issues have moderate to low development needs.

Target fabrication and injection rank second and fourth, respectively, primarily because of the newness of the technology. Being simpler than hohlraum targets, direct drive targets should be somewhat easier to fabricate.

The reactor chamber appears to have fewer development problems than the driver/target systems. The key issues here are sustained leak tightness and erosion. The first depends on the allowable helium density in the target chamber, which will certainly be much higher than the allowable xenon density, and on the pumping capacity of the vacuum system.

The final optics concerns rank fifth in development priority. Final optics problems center around pointing stability and neutron damage. The last could be a serious problem if lifetimes are much less than our estimates.

The reactor building, although very large, is technically fairly credible. Key issues are cost, vacuum maintenance, dimensional stability, and activation from scattered neutrons.

The remaining issues (i.e., Li_2O transport, IHX, steam generator, shielding, and power conversion) are all quite credible today and require little costly development.

7.3 GENERIC IFE ISSUES

The four generic issues were also evaluated using the criteria in Table 7.1, but were not ranked in priority as the power plant issues listed in Tables 7.2 and 7.3. All of the generic issues are critical in that they impact all elements of IFE power plant development. Innovations in targets, or discoveries from reactor modeling, for example, could move the program in totally unexpected directions. For this reason, lead times are considered long so that results can impact the program before long-term commitments or premature down-selections are made.

Table 7.3. SOMBRERO Development Priorities

Item	Current Technical Credibility	Development Needs	Devel. Priority
Driver	Low	High	1
Target Fabrication	Low	High	2
Reactor Chamber	Moderate	Moderate	3
Target Injection	Moderate	Moderate	4
Final Optics	Moderate	Moderate	5
Reactor Building	Moderate	Moderate	6
Li_2O Transport	High	Low	7
IHX	High	Low	8
Steam Generator	High	Low	9
Shielding	High	Low	10
Power Conversion	High	Low	11

Some interesting conclusions can be reached by examining the detailed entries in Chapter 7. For example, while the overall urgency is fairly low for reactor modeling, criticality is high and lead time is long. Development cost, however, is very low compared to other items. This suggests that an on-going, low-level effort in reactor modeling is warranted so that results can influence the IFE development program.

Low-activity, neutron-resistant materials must be vigorously pursued without delay at a fairly high level unless a commitment is made to reactor designs that have thick "healable" flowing liquid or granule blankets like HYLIFE,[2] HYLIFE-II,[5] Cascade[11] or LIFE.[17] A main attraction for fusion is the ability to design reactors with low radioactivity and little radioactive waste.

Remote maintenance, while critical, can borrow from other programs. Effort is required, however, to tailor it to the IFE program.

8.0 ECONOMIC ASSESSMENT

8.1 INTRODUCTION

After completing the conceptual designs for the Osiris and SOMBRERO power plants, cost estimates were made for the point designs, and cost scaling relationships were developed and incorporated into systems economic codes for the two power plants. These codes were then used to do parametric studies of the two designs to determine the cost of electricity (COE) as a function of design and operating parameters. The figure of merit used in our economic assessment is the constant dollar COE, which is dominated by the capital cost of the plant. The cost comparisons are most useful for identifying the most attractive operating space.

8.2 RESULTS FOR REFERENCE DESIGNS

Table 8.1 gives the capital costs, unit capital cost, and COE for the reference designs. The direct capital cost and COE of the SOMBRERO plant are nearly 20% higher than Osiris. The difference is largely attributable to the larger fusion power and gross electric power required by SOMBRERO to generate the same 1000 MWe output. In addition, the cost of the SOMBRERO reactor building is significantly larger than the Osiris reactor building due to locating the final optics 50 m from the target. The difference in the cost of reactor buildings is ~$110 M, which is about 40% of the total difference in the direct capital costs of the two plants.

8.3 RESULTS OF PARAMETRIC STUDIES FOR OSIRIS AND SOMBRERO

Parametric studies were carried out to determine the COE for different

- operating points (driver energy, chamber rep-rate, etc.),
- assumptions on target performance, and
- net electric power levels.

The COE as a function of driver energy is shown in Fig. 8.1 for both Osiris and SOMBRERO. For Osiris, the minimum COE occurs at a driver energy of 2.5 MJ. The rep-rate at E = 2.5 MJ is 16 Hz, which is probably too high for operation of the Osiris chamber. Increasing the driver energy to 3.5 MJ reduces the rep-rate to a manageable 8.6 Hz. The COE at this point is 5.37 ¢/kWh, only 2% higher than the minimum COE. The COE of the reference point design at E = 5 MJ is 5.61 ¢/kWh, less than 5% higher than the minimum COE and 3% higher than the 3.5 MJ case.

Table 8.1. Capital Costs, Unit Costs, and Cost of Electricity for Reference Designs (1991 $)

		Osiris	SOMBRERO
Direct Capital Costs			
20	Land and Land Rights	11.6	10.5
21	Structures and Site Facilities	137.6	276.1
22	Reactor Plant Equip.	504.3	615.5
23	Electric Plant Equip.	225.8	256.3
24	Turbine Plant Equip.	66.2	70.0
25	Miscellaneous Plant Equip.	18.5	19.9
26	Heat Rejection Systems	44.7	52.0
27	Driver Equipment	587.5	579.1
	Total Direct Cost	**1596**	**1879**
Indirect Capital Costs (M$)			
91	Construction Services and Equipment	192	225
92	Home Office Engineering and Services	83	98
93	Field Office Engineering and Services	96	113
94	Owners Cost	295	347
96	Project Contingency	391	461
	Total	**1057**	**1244**
Time Related Costs (M$)			
97	Interest During Construction	438	516
98	Escalation During Construction	0	0
	Total	**438**	**516**
Total Capital Cost (M$)		**3091**	**3639**
Unit Capital Cost ($/kWe-gross)		**2743**	**2678**
Unit Capital Cost ($/kWe-net)		**3091**	**3639**
Constant Dollar Cost of Electricity (¢/kWh)			
	Return on Capital	4.54	5.35
	Operation and Maintenance	1.00	1.25
	Fuel	0.02	0.02
	Decommissioning	0.05	0.05
	Total	**5.61**	**6.67**

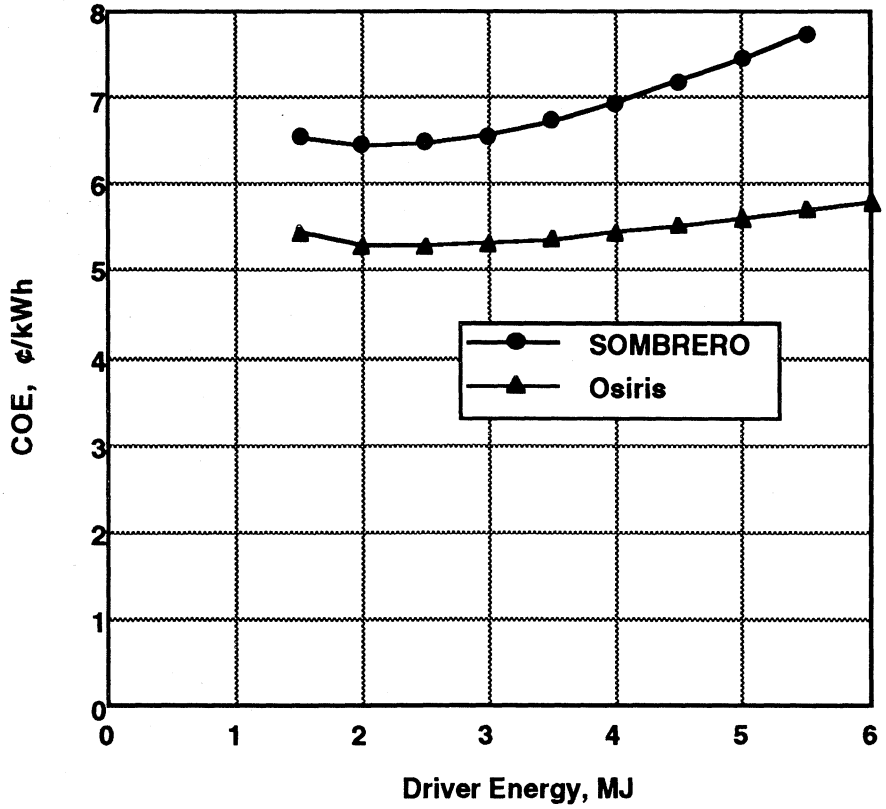

Fig. 8.1. COE vs. driver energy for 1000 MWe power plants.

For SOMBRERO, the minimum COE is 6.45 ¢/kWh, which occurs at a driver energy of 2.0 MJ. The rep-rate at E = 2 MJ is 15 Hz. We believe that the SOMBRERO chamber conditions could be reestablished at this frequency, although operating at this rep-rate puts additional stress on the target injection and tracking system. The COE of the reference point design at E = 3.4 MJ is 6.67 ¢/kWh, about 3% higher than the minimum COE.

The results of the parametric studies are summarized in Table 8.2. With optimistic target gain assumptions, the minimum COE is about 4-9% lower (Osiris result given first), and with conservative target gain assumptions, the COE is about 5-15% higher than the higher rep-rate design using base case assumptions. Increasing the net power to 1500 MWe reduces the COE by 17-15%, and reducing the net electric power to 500 MWe increases the COE by 43-38%.

Table 8.2. Summary of Results of Parametric Studies Constant Dollar COE (¢/kWh)

	Osiris	SOMBRERO
Reference Design	5.61	6.67
Higher Rep-rate Designs	5.37	6.45
Conservative Gain Curve	5.64	7.44
Optimistic Gain Curve	5.15	5.89
Lower Net Power (500 MWe)	7.69	8.88
Higher Net Power (1500 MWe)	4.48	5.49

8.4 CONCLUSIONS

In the context of the level of accuracy of our cost estimates, the 20% difference in the COE is not important enough to eliminate the KrF-driven design from further development. In fact, we note that the COEs for these designs are both quite competitive with cost estimates made for ARIES-I and ARIES-II magnetic fusion energy designs, which reported constant (1988$) dollar COEs of 8.11 ¢/kWh and 6.69 ¢/kWh, respectively.[18] While we have not done a careful comparison of the IFE designs with the MFE designs, it is interesting to note that the cost of the drivers (at ~$600 M) is on the same order as the $500 M sum of costs for the magnets ($339 M), current heating ($108 M), and energy storage ($51 M) for ARIES-I (ARIES costs in 1988$). The COEs for Osiris and SOMBRERO are higher than the projected COEs for the 1200 MWe Improved PWR (4.3 ¢/kWh) and 1200 MWe Advanced PWR (4.5 ¢/kWh), but they are competitive with the projected COE from future coal plants (5.8 ¢/kWh) and "best experience" present day PWRs (5.4 ¢/kWh).[19]

9.0 COMPARISON OF OSIRIS AND SOMBRERO DESIGNS

9.1 INTRODUCTION

Chapter 9 gives quantitative comparisons of design features and operating parameters of Osiris and SOMBRERO. Some of the key parameters and features are compared in Table 9.1. No attempt was made to rate and rank the two concepts using a numerical scoring system as in studies such as BCSS[63] and ESECOM.[64] Both designs have major uncertainties and require significant technology development. At this time, there is no clear choice for the best concept. More meaningful comparisons and judgments of attractiveness can be made after some of the critical issues are addressed and the technologies are developed further.

9.2 DRIVERS

The HIB driver for the Osiris power plant operates at a higher energy but lower rep-rate than the KrF laser driver for SOMBRERO. The HIB driver efficiency is considerably higher, which results in less driver power consumption and correspondingly less gross electric power required to produce 1000 MWe of net power. Both drivers are far larger than present-day experiments and require a great deal of development work. Predicted driver efficiencies for both driver are based on extrapolations of experimental data and are probably achievable with engineering development.

9.3 TARGETS

Osiris uses an indirect drive target that produces a gain of 87 at a driver energy of 5 MJ giving a yield of 432 MJ. The illumination geometry is two-sided with 6 beams from each side. The SOMBRERO target is a direct drive target using uniform illumination with 60 beams delivering a total of 3.4 MJ. The target gain in this case is 118 for a yield of 400 MJ.

9.4 CHAMBER DESIGNS

Table 9.1 contrasts the key design features of the Osiris and SOMBRERO chamber designs. Osiris and SOMBRERO use different methods to protect the first wall material. The Osiris design uses a sacrificial layer of molten Flibe which must be replaced between shots. The SOMBRERO first wall is protected from target x rays and ion debris by 0.5 torr of Xe, which spreads out the energy deposition time and prevents vaporization of the C/C composite. The two

Table 9.1. Comparison of Key Design Features for Osiris and SOMBRERO

	Osiris	SOMBRERO
Driver		
Driver Energy (MJ)	5.0	3.4
Rep-Rate (Hz)	4.6	6.7
Driver Efficiency	28.2	7.5
Target		
Type	Indirect Drive	Direct Drive
Target Gain	86.5	118
Yield (MJ)	432	400
Chamber Design		
First Wall Material	Woven Graphite Fabric	4-D C/C Composite
X-ray and Debris Protection	Liquid Flibe	3.25 torr-m of Xe
First Wall Radius, m	3.5	6.5
Estimated First Wall Life (fpy)	1.8	5
Breeding Material	Molten Flibe	Li_2O Granules
Blanket Thickness (m)	0.7	1.0
Tritium Breeding Ratio	1.24	1.25
Overall Energy Multiplication	1.26	1.08
Chamber Outer Wall Material	C/C Composite	C/C Composite
Outer Wall Radius (m)	6.5	7.5
Power Conversion System		
Primary Coolant	Flibe	He w/ Li_2O granules
Temperature Range (°C)	500 - 650	550 - 700
Intermediate Coolant	Lead	Lead
Temperature Range (°C)	400 - 600	400 - 600
Secondary Coolant	Water / Steam	Water / Steam
Temperature Range (°C)	286 - 538	286 - 538
Cycle	Double Reheat	Double Reheat
Peak Steam Pressure (MPa)	24	24
Power Conversion Eff. (%)	45	47
Power Balance		
Fusion Power (MW)	1987	2677
Total Thermal Power (MWt)	2504	2891
Gross Electric Power (MWe)	1127	1359
Driver Power (MWe)	82	304
Auxiliary Power (MWe)	45	55
Net Electric Power (MWe)	1000	1000

design choices were driven by the great difference in the required gas pressures assumed for final beam transport the two drivers. Both chamber designs assume carbon-based structural materials, which require further development.

Blankets used in fusion reactors must provide heat transport and tritium breeding; in addition, they should minimize potential hazards resulting from activation and chemical hazards. The blankets used in Osiris and SOMBRERO use different approaches to meet these design goals. Osiris uses flowing molten Flibe channels for breeding and heat transport, as well as for replenishing the sacrificial protection layer for the first wall. SOMBRERO, in contrast, uses a fluidized flow of solid Li_2O particles in a helium purge gas to get the advantages of both a solid breeder and a moving blanket.

Both Osiris and SOMBRERO have a very robust breeding ratio. However, because there is a large quantity of Be in the Flibe, the energy multiplication is higher than in Li_2O. First wall damage, He production, and estimated chamber life are all functions of the chamber radius. Since the first wall radius in Osiris is 3.5 m as compared to 6.5 m in SOMBRERO, the damage rate in Osiris is higher, and the first wall lifetime is lower. There is considerable uncertainty in the estimated first wall lifetime for both systems, because of the scarcity of damage data for the materials in question.

9.5 POWER CONVERSION SYSTEMS

Table 9.1 contrasts the power conversion system parameters for Osiris and SOMBRERO. Both reactors use a lead intermediate loop to reduce tritium flow to the steam in the secondary loop and a double reheat steam cycle to maximize the power conversion efficiency. The power conversion efficiency for SOMBRERO is slightly higher, because waste heat from the laser amplifiers is used in feedwater heaters for the secondary loop. The SOMBRERO reactor requires a larger gross power than Osiris, because the HIB driver requires less power than the KrF laser for a given net electrical power.

9.6 RESULTS OF ASSESSMENT STUDIES

Comparisons of the environmental and safety aspects, the RAM analysis, technology development requirements, and the economic assessments are given in Sections 5, 6, 7, and 8 of the Overview, respectively.

10.0 CONCLUSIONS AND RECOMMENDATIONS

10.1 INTRODUCTION

The primary objective of the IFE Reactor Design Studies was to provide the Department of Energy with an evaluation of the potential of inertial fusion for electric power production. Based on the results of these studies, we conclude that IFE has the potential of producing technically credible designs with environmental, safety, and economics characteristics that are every bit as attractive as magnetic fusion. Realizing this potential will require additional research and development on target physics, chamber design, target production and injection systems, and drivers.

10.2 OSIRIS POWER PLANT

Osiris Chamber

The Osiris chamber features a very compact, low-activation chamber that uses ceramic material in a flexible, leak-tolerant configuration. The blanket consists of a porous carbon fabric filled with Flibe for cooling and tritium breeding. The Flibe coats the fabric surface, and vaporized Flibe is condensed in a pool at the bottom. The materials and technology needed to construct this blanket exist today. The Osiris vacuum vessel is protected from neutron damage and is a lifetime component. The fabric first wall is replaced periodically (about every two years), but the procedure for doing so is very simple – the entire blanket assembly is drained of Flibe and lifted out the top of the vacuum vessel.

We recommend additional research and development on several aspects of the Osiris design to address unresolved issues, as described below.

First Wall Design. While the materials exist to construct the fabric first wall, research is needed to determine the correct fabric weave to control the flow of Flibe through the fabric first wall. Since Flibe does not wet carbon, it may be difficult to maintain a uniform coating on the first wall. Effects of fabric design parameters and the possibility of using thin wettable metallic coating should be examined. The lifetime of the first wall will be determined by neutron damage and chemical corrosion by free fluorine; the lifetime limits are uncertain and require more research.

Chamber Dynamics. Osiris uses a spray of Flibe at the cold-leg temperature to condense the material vaporized on each shot. Two-dimensional modeling of vapor flow and benchmark experiments are needed. Calculations indicate that recombination of the Flibe after dissociation by the fusion energy pulse will not limit the rep-rate. This should be verified experimentally.

Tritium Recovery and Control. A more detailed analysis of the amount of tritium that can be recovered directly from the Osiris chamber is needed. If all the tritium can not be released by the cascading flow behind the blanket, vacuum disengagers as used in HYLIFE-II will be needed. Vacuum pumping along the beam lines near the chamber are need to prevent the flow of tritium and other radioactive materials into the accelerator. Modeling and small-scale experiments are needed to demonstrate the viability of maintaining the required vacuum conditions.

Vacuum Chamber Structure. The Osiris vacuum chamber is made of carbon/carbon (C/C) structures. The technology to produce large composite structures needs further development.

HIB Driver

The design of the induction linac driver emphasized cost reduction. Costs were reduced by operating at the maximum transportable current in order to minimize length. The 5 MJ driver uses a propagation mode in the accelerator with constant beam radius, quadrupole strength, and quad length – all of which encourage cost-reducing mass production. Twelve beams of Xe^{+1} are accelerated through common cores to a final voltage of 4.8 GeV. Compact Nb_3Sn superconducting quads are used in a standard FODO propagation mode. Complexities from beam combination, separation, or recirculation are avoided. The beams are almost completely neutralized with co-injected electrons just prior to entering the chamber. This gives a relatively small spot size (2.3 mm) and a target gain of ~87. The high-current, low voltage configuration of the accelerator leads to a relatively low cost ($120/J direct cost) design. The high driver efficiency (28%) gives a low recirculating power fraction of only 7%.

We recommend continued development of heavy-ion driver system technology in several areas. Near-term, small-scale research should continue in the following areas:

Injector Development. Because such a large fraction of driver elements are located early in the driver, significant cost savings are possible with improved injector performance. Increasing the injector current and/or voltage would reduce the length and required elements for the low-energy section of the driver by greatly increasing the acceleration gradient allowed by the velocity-tilt limit. Because the normalized emittance for the entire driver and the emittance contribution to the achievable spot size at the target are set by the injector, it is imperative that low-emittance, high-current injectors be demonstrated.

Quadrupole Array Development. Uncertainties in driver cost and transportable current at low energies could be greatly reduced by a prototype design program for superconducting quadrupole arrays. Transportable current at low driver energies is determined by the limits on how short a high-quality quadrupole can be and by how close quadrupoles can be placed without destructive interference of the end fields. Careful design and measurement of short quadrupoles would better establish these limits. In addition, design and demonstration of a single compact

quadrupole array would greatly increase the credibility of size and cost estimates for the entire driver.

Larger experimental programs, such as ILSE, are needed to verify beam scaling and could establish the feasibility of aggressive design options. Recommended experiments are:

Current Transport Limits. MBE-4 has demonstrated the ability to accelerate multiple beams, but a longer driver such as ILSE would also demonstrate high-current transport, scaling of transportable current with voltage, and velocity-tilt limits on acceleration gradients.

Beam Combination and Separation Experiments. Transport and combination or splitting magnets could be added to the end of an ILSE-like accelerator to examine the achievable beam quality after beam combination or separation. As we have shown, neither of these options is necessary for heavy-ion drivers to be credible, but both options could lead to cost reductions once their feasibility is proven.

Beam Bending Experiments. There is great uncertainty concerning the feasibility or performance of a recirculator. One set of uncertainties concerns loss of beam quality in the bending magnets, another concerns resonant instabilities, and a third set concerns maintaining vacuum quality. Scalable experiments on an ILSE-scale device with either a recirculating accelerator section or a loop of quadrupoles and dipoles following the accelerator could give a great deal of information on the feasibility of recirculating drivers. As with beam combination and separation, recirculation is not necessary for heavy-ion drivers, but it could lead to cost reductions.

Drift Compression and Focusing Experiments. A proven accelerator will still need proven final focusing and transport to be of use as an IFE driver. Modeling and scaling of the behavior of high-energy, high-current beams under drift compression and final focusing will greatly benefit from scaled experiments with lower-energy beams.

Power Conversion and Balance of Plant (BOP)

The power conversion system for Osiris is a conventional super-critical steam cycle giving 45% efficiency. A low-pressure liquid lead intermediate heat exchanger provides pressure isolation and prevents the possibility of direct contact between the primary coolant, which contains tritium and other activated material, and the steam system. It appears that the BOP design for Osiris is technically viable, and there do not appear to be any issues that can not be adequately resolved.

The use of an intermediate heat transport loop was adopted for this study as a conservative measure. However, to reduce plant cost and complexity associated with a intermediate coolant and additional equipment, the use of a duplex-tube steam generator approach should be evaluated in more detail. If found appropriate, the technology for this kind of steam generator should be developed in conjunction with the Advanced Liquid Metal Reactors program.

10.3 SOMBRERO POWER PLANT

SOMBRERO Chamber

SOMBRERO chamber is an attractive, high temperature chamber design. It avoids the problem of first wall vaporization by protecting the wall with a low density inert gas (xenon). The first wall and chamber are constructed of a low-activation C/C composite. Granules of Li_2O flow though the chamber and are circulated as the primary coolant. The design retains the advantages of solid breeders while eliminating the problems associated with static blankets. The feasibility of the flowing blanket and fluidized recirculation are within the capabilities of existing industrial practice. The chamber is constructed of 12 independent first wall and blanket modules that must be replaced approximately every five years.

Additional research and development are recommended for SOMBRERO. Some of the key areas are listed below.

First Wall and Chamber Design. Experimental verification of the effectiveness of the first wall protection scheme is recommended. The development of the capability to manufacture larger C/C composite structures is essential to the design concept. Radiation damage tests with composite materials to determine material lifetime the effects on thermal conductivity are needed. A materials development program for this class of materials is needed for both IFE and MFE.

Laser Propagation. If the xenon gas density is too high, breakdown can occur which would reduce the amount of energy delivered to the target. Experiments to quantify the limits on the density of the gas are needed at the correct wavelength and intensity. The implications on target performance if breakdown occurs near the target also need additional study.

Flowing Blanket. Several aspects of the flowing breeding blanket would benefit from further study. Additional experiments on the heat transfer capabilities of the flowing bed examining a wider range to the operating variables and materials should be carried out. The issues of granule break-up and erosion of the blanket and heat transfer components need study.

Tritium Control. Since tritium is present in the xenon gas that fills the reactor building, it is essential that the building walls do not absorb tritium. Verification of the ability of coatings to prevent absorption is needed.

Power Conversion and BOP

The power conversion system for SOMBRERO is the same as for Osiris, except the intermediate heat exchanger has Li_2O granules instead of Flibe on the primary loop side. The system utilizes waste heat from the laser amplifiers to increase the gross conversion efficiency from 45 to 47%. The balance-of-plant design for SOMBRERO appears to be technically viable. Conceptual solutions have been identified for the major issues. The interface between the laser and

the chamber (i.e., the optical train needed to deliver the beams) places significant demands on the design and construction of the reactor building.

As with the Osiris design, a closer look at the feasibility of a duplex wall steam generator (instead of using an intermediate heat exchanger) is advised.

The layout of the final optics adopted for this design is determined by the requirement for reasonable lifetimes of the mirrors. Grazing incidence metal mirrors (GIMMs) have been chosen as the final optics with the dielectric focusing mirrors located out of the line of sight. There are almost no data on radiation damage of either metal or dielectric optics in high energy neutron fluences. It is clear that the damage threshold of these optics under neutron illumination is one of the major uncertainties in this design. If the optics were to have higher fluence tolerances than assumed, then the optics could be placed closer to the target and the whole structure reduced in size. This could reduce the cost of the SOMBRERO reactor building significantly. Thus obtaining radiation damage data is critical.

The CaF windows located on the floor of the reactor building separate the reactor building environment from the beam handling area while letting the laser beams pass through with minimum absorption. While these windows are not in the direct line of sight for neutron irradiation, they will receive some scattered neutron fluence. Neutron damage data is also needed for these optics.

KrF Driver

The KrF driver system we have designed has an overall efficiency of 7.5% and the use of waste heat from the amplifiers increases the power conversion efficiency by ~2%. (This is equivalent to an effective laser efficiency of > 9%.) We have achieved this high KrF system efficiency by

1) careful overall optimization of the final amplifier design parameters,
2) use of high pump rate kinetics to achieve high intrinsic efficiency,
3) use of low inductance e-beam system design to allow low rise/fall time losses,
4) use of a recently patented and demonstrated plasma cathode in the e-beam that is capable of efficiencies limited only by the gas/foil albedo, and
5) operation at high Joules/liter, which allows efficient waste heat utilization.

Our design uses 60 kJ amplifier cavities that are pumped for 600 ns from two sides with 600 kV, 40 A/cm^2 e-beams that are 1×2 meter in dimension. The cavities operate in a 2-pass extraction mode. This is a relatively small size that has high efficiency due to low amplified stimulated emission, excellent fill factor, and low flow power. The small size promises to keep development cost at a minimum for full-size demonstration of key components.

We feel our design represents the best of the possible approaches, given current data on the KrF system. We have not extrapolated physics, but we have made reasonable and defensible

projections for technology development, based on scaling demonstrated technology. Our approach also has the advantage of representing sensible evolution of the technologies developed in Aurora (e-beam pumped 2-pass amplifiers with angular multiplexing for pulse compression), Nike (non-echelon integrated spatial incoherence for smooth beam profiles on high gain direct drive targets), and EMRLD (DoD technology for repped e-beam pumped excimers of excellent beam quality).

We recommend continued development of the KrF driver system technology in the following areas:

Repped e-Beam. The plasma cathode technology should be scaled from 10×30 cm to 1×2 m, and the design optimized for 5 to 10 Hz operation. Operation of a 1×2 m, 600 kV, 40 A/cm^2, 600 ns e-beam with cable-based pulse power should be the final milestone of this effort.

60 kJ Amplifier Module. Demonstrate 10 Hz operation with angular multiplex extraction over at least part of the 600 ns gain duration. Perform an extensive characterization of the operating parameters and develop an understanding of issues for the next generation design, particularly to extend foil lifetime.

Zooming Front End. Develop and test a front end design capable of changing aperture diameter by about two in periods of order 6 ns, with simultaneous control of the power output as required for optimum target implosion.

KrF Kinetics. Demonstrate the high intrinsic efficiency predicted by our codes for 400 kW/cm^3 pump rate for 600 ns, and thus also demonstrate the 30 J/liter design.

Neutron Effects on Optics. With a 14.1 MeV neutron test facility, develop and test designs for the grazing incidence metal mirrors and the dielectric-coated final focusing mirrors.

Cooled Optics. Develop and test designs in the 10×20 cm size operating at 5 J/cm^2 and 10 Hz in the UV.

Lifetime Testing of Critical Components. Besides the neutron effects and the optics fluence and average power testing, there are a number of other components, such as the e-beam cathodes, pulse power switches, and so forth that should be tested.

Overall System Design. The present program was a minimal size effort to accomplish the goals; there is much that should be worked out to the next level of detail to improve the confidence level and guide the subsequent developments.

10.4 TARGET SYSTEMS

Target Production

The target production facility design was motivated by the objectives of high reliability, high safety, and low capital cost. The facility uses controlled microencapsulation for shell production, fuel filling by cryogenic injection, and layer formation by pulsed laser heating and temperature-controlled gas jets. The building area required for target fabrication is quite compact. The production process is expected to have high reliability because there is 100% redundancy in the production lines. The total tritium inventory is low (~300 g) as a result of using rapid fill and layering techniques.

The proposed technologies are speculative and require significant technology development.

Shell Production. Controlled microencapsulation has been demonstrated for small-sized capsules. The process must be scaled up to demonstrate that high quality can be maintained for larger targets characteristic of the high yield targets used for power plants.

Fuel Filling. The proposed cryogenic fill technique has a great advantage in that the fill time is very short (~minutes), and thus the tritium inventory associated with the fill step is small. The technology has not been demonstrated and significant uncertainties exist. Small-scale experiments should be carried out to begin addressing the issues associated with this process.

Fuel Layering. The use of pulsed lasers and cold gas jets has been demonstrated for small targets. Development is needed to see if this technique can be scaled up to be used with larger targets and thicker fuel layers.

Target Injection, Tracking and Beam Pointing

Existing gas gun technology can meet the acceleration and positioning requirements of the IFE applications. The proposed design uses a sabot to protect the target from damage during the acceleration processes. Laser Doppler interferometer and laser tracking station are used to monitor the target trajectory and can provide pointing information in enough time to actively point the beams for each shot. The tracking and pointing requirements can be met with existing technologies. The most critical issues have to do with operating the injector with cryogenic targets.

Small-scale tests should be carried out to demonstrate the integration of the technologies required for target injection, tracking, and beam pointing. The test could be conducted in a phased approach by first developing the gas gun injector, adding tracking systems, and finally demonstrating beam pointing and interception of a target with a low energy ion or laser beams. Operation with cryogenic targets, but not necessarily DT, will be required.

Target Survivability

The target is protected from physical contact with the accelerator by a sabot. Once the target leaves the accelerator, the sabot flies off. As the target travels through the chamber, it is subjected to convective and radiative heat loads. For indirect drive targets, the hohlraum provides a thermal barrier to protect the fuel capsule. Direct drive targets will have to remain in the sabot for a longer time or incorporate additional thermal protection (e.g., a sacrificial layer of frozen gas on the outer surface of the capsule), especially when used in high temperature chambers such as SOMBRERO. More work is needed to demonstrate the integrity of the DT fuel layer and capsule during acceleration and transit through the chamber.

Experiments are needed to develop appropriate sabot designs that can protect the capsule during acceleration. The integrity of cryogenic hydrogen layers should also be examined to determine acceleration limits for targets. Experiments with schemes to protect the targets from heat loads during injection are also needed.

10.5 ENVIRONMENTAL AND SAFETY ASSESSMENT

Both Osiris and SOMBRERO have attractive environmental and safety characteristics. Both achieve a level of safety assurance of one, and the chamber, breeder, and shielding materials will qualify for disposal as Class A or C low level waste. These results are due to the use of only low-activation materials for the first walls, breeding blankets, and chamber structures. As previously mentioned, minimizing the tritium inventory in the target factory is also an important aspect in achieving the high safety rating.

To realize potential environmental and safety advantages of these designs, the low-activation structural materials used for the SOMBRERO first wall, blanket, and chamber structure and for the Osiris vacuum chamber will require significant technology development. The carbon fabric used for the Osiris first wall and blanket is currently available, but as discussed above, development the proper weave density for flow control is need.

10.6 RELIABILITY, AVAILABILITY, AND MAINTAINABILITY

At a conceptual level of evaluation, the remote maintenance of the Osiris and SOMBRERO reactors appears feasible. However, a detailed evaluation of the remote replacement or refurbishment of the reactor components should be performed to identify the development needs for any special remote maintenance equipment. In addition, "design for remote maintainability" should be factored into the program from the beginning of conceptual designs rather than retrofitting at later stages.

At this stage of the IFE reactor development, a definitive assessment of the reliability, availability, and maintainability (RAM) can not be performed until an in-depth evaluation of the key systems and components is made. In addition, in-depth evaluations are needed on the integrated design and performance of the driver, target, reactor, and the balance-of-plant.

An overall plant availability goal of 75% is assumed here for the IFE reactor plants so as to be comparable to other large electric power generating systems. To be able to meet this target goal, it appears that both concepts require significant improvements in the availability of the constituent systems and components. A detailed RAM assessment is needed to identify the extent of the improvement and to aid in planning future development efforts.

10.7 ECONOMIC ASSESSMENTS

The estimated cost of electricity (COE) for the SOMBRERO power plant is about 19% higher than the COE for the Osiris power plant. The economics for both plants are attractive compared to previous inertial and magnetic fusion reactor designs. The use of low-activation materials and low volatile tritium inventory eliminates the need for N-stamp materials and reduces the estimated construction costs.

The attractive economics are the result of properly integrating the proposed technologies (lower cost heavy ion driver, more efficient KrF laser, good target gain performance, etc.). Continued systems analysis is useful to help identify those areas with high leverage for affecting system performance and bottom line costs. A continuing effort in power plant systems analysis that incorporates the latest information on reactor, driver, and target technologies and performance is recommended. Further work is also recommended to normalize the cost estimates with other IFE and MFE studies so that they can be compared on a more consistent basis. For high leverage systems and subsystems, more detailed designs and cost estimates are warranted.

11.0 REFERENCES

1 R.C. Davidson, C.C. Baker, R.O. Bangerter, E.C. Brolin, D.R. Cohn, D.L. Cook, D.J. Dudziak, D.B. Harris, R.A. Krakowski, T.E. Shannon, W.E. Stacey, C.P. Verdon, "Inertial Confinement Fusion Reactor Design Studies Recommended Guidelines," (Sept. 1990).

2 M.J. Monlser, "The HYLIFE Concept: Electricity form Laser Fusion," *Trans. Am. Nucl. Soc.*, **30**, 21 (1978). Also J.A. Blink et al., "The High-Yield Lithium-Injection Fusion Energy (HYLIFE) Reactor, Lawrence Livermore National Laboratory, UCID-53559 (1985).

3 B. Badger et al., "HIBALL-II - An Improved Heavy-Ion Beam Driven Fusion Reactor Study," University of Wisconsin Fusion Technology Institute, UWFDM-625 (Dec. 1984).

4 M.J. Monsler, "New Inertial Fusion Reactor Concepts - Pulse*Star," Laser Program Annual Report, Lawrence Livermore National Laboratory, UCRL-50021-82 (1983).

5 R.W. Moir, "HYLIFE-II Inertial Confinement Fusion Reactor Design," Lawrence Livermore National Laboratory, UCRL-JC-103816 (Oct. 1990).

6 J. Hovingh et al., "Heavy-Ion Linear Induction Accelerators as Drivers for Inertial Fusion Power Plants," *Fusion Technol.*, **13**, No. 2, 262 (Feb. 1988).

7 W.M. Polansky, "U.S. Accelerator Research Program for Heavy-Ion Fusion," *Fusion Technol.*, **13**, No. 2, 202 (Feb. 1988).

8 M.J. Monsler, "The Potential for Reducing the Cost of a Heavy-Ion Accelerator for ICF," Final Report PO #9056305, Submitted to Lawrence Livermore National Laboratory (Feb. 1987).

9 D.K. Sze et al., "Gravity Circulated Blanket Design for a Tokamak Fusion Reactor," *Proc. 2nd Topical Meeting on the Technology of Controlled Nuclear Fusion*, Richland, WA (1976).

10 R.W. Conn et al., "SOLASE - A Conceptual Laser Fusion Reactor Design," UWFDM-220, Fusion Research Program, Nuclear Engineering Dept., Univ. of Wisconsin, Madison (Dec. 1977).

11 J.H. PITTS, "Cascade: A Centrifuged-Action Solid Breeder Reaction Chamber," *Nucl. Technology/Fusion*, **4**, 967 (1983). also J.H. Pitts, "The Cascade Inertial Confinement Fusion Reactor Concept," Lawrence Livermore National Laboratory, UCRL-LR-104546 (Dec. 1990).

12 R.R. Berggren, R.L. Gibson, R.H. Lehmberg, and C.W. vonRosenberg, Jr., "Large KrF Lasers as High-Brightness, High-Energy Sources," also D.B. Harris, et al. "Strengths and Weaknesses of KrF Lasers for ICF Applications Learned from the AURORA Laser," IAEA Technical Committee Meeting on Drivers for Inertial Confinement Fusion, Osaka, Japan, (April 15-19, 1991).

13 M. McGeoch, "A High Current Density Non-Closing Plasma Cathode," *J. Appl. Phys*, **71** (3), 1163 (Feb. 1992); also U.S. Patent No. 5,003,226.

14 H. Rieger et al., "Cryogenic Laser Target Fabrication System Directly Operable Inside a Target Chamber," Lawrence Livermore National Laboratory, UCRL-83079 (1979).

15 M.R. Lee and J. Sesak, "Control System Requirement Extracted from the Stanlab Hardware Specification, EM-238," Lockheed Missiles and Space Co., F185873 (1988).

16 D. Orvis et al., "Guidebook for RAM Analysis," General Atomics Company Technical Report, ONWI-334 (April 1981).

17 R.F. Bourque, "ICF Reactor Chambers with Rotating Liquid Blankets," *Proc. 14th IEEE/NPSS Symposium on Fusion Engineering* (Sept. 30 - Oct. 3, 1991, San Diego, CA) **2**, 642 (1992).

18 R.L. Miller, R. A. Krakowski, and ARIES Team, "Options and Optimizations for Tokamak Reactors: ARIES," *Fusion Technol.*, **19**, 802 (May 1991).

19 J.G. Delene, "Updated Comparison of Economics of Fusion Reactors with Advanced Fission Reactors," *Fusion Technol.*, **19**, 807 (May 1991).

20 D.L. Smith et al., "Blanket Comparison and Selection Study - Final Report," Argonne National Laboratory, ANL / FPP-84-1 (Sept. 1984).

21 J.P. Holdren et al., "Report of the Senior Committee on Environmental, Safety, and Economic Aspects of Magnetic Fusion Energy," Lawrence Livermore National Laboratory, UCRL-53766 (Sept. 1989).

GPO 786-532/99151